

## RESEARCH ARTICLE

# Direct estimation of catchment response time parameters in medium to large catchments using observed streamflow data

O.J. Gericke<sup>1,2</sup> | J.C. Smithers<sup>2,3,4</sup>

<sup>1</sup>Unit for Sustainable Water and Environment, Department of Civil Engineering, Central University of Technology, Free State, Bloemfontein, South Africa

<sup>2</sup>Bioresources Engineering, School of Engineering, University of KwaZulu-Natal, Pietermaritzburg, South Africa

<sup>3</sup>Jeffares & Green (Pty) Ltd, 6 Pin Oak Avenue, Hilton, Pietermaritzburg, South Africa

<sup>4</sup>National Centre for Engineering in Agriculture, University of Southern Queensland, Toowoomba, Australia

**Correspondence**

Gericke, Ockert, Department of Civil Engineering, Central University of Technology, Free State, Bloemfontein, South Africa.  
Email: jgericke@cut.ac.za

**Funding information**

National Research Foundation (NRF), University of KwaZulu-Natal (UKZN) and Central University of Technology, Free State (CUT FS)

**Abstract**

In single-event deterministic design flood estimation methods, estimates of the peak discharge are based on a single and representative catchment response time parameter. In small catchments, a simplified convolution process between a single-observed hyetograph and hydrograph is generally used to estimate time parameters such as the time to peak ( $T_p$ ), time of concentration ( $T_c$ ), and lag time ( $T_l$ ) to reflect the “observed” catchment response time. However, such simplification is neither practical nor applicable in medium to large heterogeneous catchments, where antecedent moisture from previous rainfall events and spatially non-uniform rainfall hyetographs can result in multi-peaked hydrographs. In addition, the paucity of rainfall data at sub-daily timescales further limits the reliable estimation of catchment responses using observed hyetographs and hydrographs at these catchment scales. This paper presents the development of a new and consistent approach to estimate catchment response times, expressed as the time to peak ( $T_{Px}$ ) obtained directly from observed streamflow data. The relationships between catchment response time parameters and conceptualised triangular-shaped hydrograph approximations and linear catchment response functions are investigated in four climatologically regions of South Africa. Flood event characteristics using primary streamflow data from 74 flow-gauging stations were extracted and analysed to derive unique relationships between peak discharge, baseflow, direct runoff, and catchment response time in terms of  $T_{Px}$ . The  $T_{Px}$  parameters are estimated from observed streamflow data using three different methods: (a) duration of total net rise of a multi-peaked hydrograph, (b) triangular-shaped direct runoff hydrograph approximations, and (c) linear catchment response functions. The results show that for design hydrology and for the derivation of empirical equations to estimate catchment response times in ungauged catchments, the catchment  $T_{Px}$  should be estimated from both the use of an average catchment  $T_{Px}$  value computed using either Methods (a) or (b) and a linear catchment response function as used in Method (c). The use of the different methods in combination is not only practical but is also objective and has consistent results.

**KEYWORDS**

baseflow, catchment response time, direct runoff, large catchments, time to peak

## 1 | INTRODUCTION

In single-event deterministic design flood estimation methods, estimates of the peak discharge are based on a single and representative catchment response time parameter, and the catchment is at an “average condition” and the hazard or risk associated with a specific event is reflected by the joint-probability of the 1:  $T$ -year rainfall and 1:  $T$ -year flood event (SANRAL, 2013). Catchment response time parameters such as the time to peak ( $T_p$ ), time of

concentration ( $T_c$ ), and lag time ( $T_l$ ) serve as a fundamental input to all methods of estimating peak discharges in ungauged catchments; hence, errors in estimated catchment response time directly impact on estimated peak discharges (McCuen, 2009; Gericke & Smithers, 2014). Bondelid et al. (1982) indicated that as much as 75% of the total error in design peak discharge estimates in ungauged catchments could be ascribed to errors in the estimation of catchment response time parameters, and Gericke and Smithers (2014) also showed that the underestimation of time parameters by

80% or more could result in the overestimation of design peak discharges of up to 200%.

Time variables describe the individual events defined on either a hyetograph or hydrograph, and a time parameter is defined by the difference between two interrelated observed time variables (McCuen, 2009). In small catchments, time parameters are estimated using a simplified convolution process between a single rainfall hyetograph and the resulting single-peaked hydrograph. Therefore, rainfall and streamflow data are required when a simplified convolution process is applied, and a synthetic transfer function is used to transform the effective runoff producing rainfall into direct runoff based on the principle of linear super-positioning, that is, multiplication, translation, and addition (Chow et al., 1988). The estimation of catchment response time parameters from observed rainfall and streamflow data in medium to large heterogeneous catchments also requires a similar convolution process to establish the temporal relationship between a catchment hyetograph, which may be derived from numerous rainfall stations, and the resulting outflow hydrograph (Gericke & Smithers, 2014). However, several problems are associated with such a simplified convolution procedure at medium to large catchment scales. Conceptually, such a procedure normally assumes that the volume of direct runoff is equal to the volume of effective rainfall, and that all rainfall prior to the start of direct runoff is regarded as initial abstraction, after which the loss rate is assumed to be constant (McCuen, 2005). Therefore, a uniform response to rainfall within a catchment is assumed, but the spatially non-uniform antecedent soil moisture conditions within the catchment, which are a consequence of both the spatially non-uniform rainfall and the heterogeneous nature of soils and land cover in the catchment, are ignored. Consequently, in contrast to small catchments with single-peaked hydrographs, the variability evident in medium to large catchments, typically results in multi-peaked hydrographs.

In addition to all above problems related to a simplified convolution process at medium to large catchment scales, the number of hydrometeorological monitoring stations, especially rainfall stations in South Africa (SA) and around the world, has declined steadily over the last few decades. According to Lorenz and Kunstmann (2012), the number of automated rainfall stations across Europe declined by nearly 50% between 1989 and 2006, whilst a more rapid decline occurred in South America. Internationally, the United States of America has witnessed one of the slowest declines. SA is no exception, and the rainfall-monitoring network has declined over recent years with the number of stations reducing from more than 2,000 in the 1970s to the current situation, where the network is no better than it was as far back as 1920 with currently less than a 1,000 stations open in a specific year (Pitman, 2011). Balme et al. (2006) also showed that a decline in the density of a rainfall-monitoring network produces a significant increase in the errors of spatial estimation of rainfall at annual scales and even larger errors at event scales for large catchments. In contrast to rainfall data, streamflow data are generally less readily available internationally, but the data quantity and quality enable it to be used directly to estimate catchment response times at medium to large catchment scales. In SA, for example, there are 708 flow-gauging station sites with more than 20 years of record available (Smithers et al., 2014).

At medium to large catchment scales, especially in SA, the use of rainfall data to estimate average catchment hyetographs, also poses several additional problems as a consequence of the following (Schmidt and Schulze, 1984; Gericke and Smithers, 2014): (a) paucity of rainfall data at sub-daily timescales, both in the number of rainfall gauges and length of the recorded series; (b) poor time synchronisation between point rainfall data sets from different gauges; (c) difficulties in measuring time parameters for individual events directly from digitised autographic records owing to difficulties in determining the start time, end time, and temporal and spatial distribution of effective rainfall over the catchment; and (d) poor time synchronised rainfall and streamflow recorders.

In a comprehensive literature review, Gericke and Smithers (2014) detailed almost 50 empirical methods developed internationally to estimate catchment response time parameters. However, the majority of these international methods are applicable to and calibrated for small catchments, with only the study of Thomas et al. (2000) applicable to medium catchment areas of up to 1,280 km<sup>2</sup>, and the studies of Johnstone and Cross (1949), Pullen (1969), Mimikou (1984), Watt and Chow (1985), and Sabol (2008) focusing on larger catchments of up to 5,000 km<sup>2</sup>. Only the method to estimate  $T_L$  implemented by Pullen (1969) was developed locally in SA, and Schmidt and Schulze (1984) also derived  $T_L$  for 12 small agricultural catchments ( $\leq 3.5$  km<sup>2</sup>) in SA and the United States. The large number of empirical time parameter equations available in practice not only results in a wide range of time parameter estimates, but these empirical equations are frequently applied outside of the regions, where they were developed. Hence, the application of such empirical time parameter equations beyond their original developmental boundaries without using local correction factors is a common practice in SA. In a recent study, Gericke and Smithers (2016) used the observed catchment response time parameters obtained from this study to derive new empirical time parameter equations in medium to large catchments. These catchment-specific or regional empirical time parameter equations resulted in improved peak discharge estimates in 60 of the 74 catchments (20 km<sup>2</sup> to 35,000 km<sup>2</sup>) situated in the study area as described in this paper.

The inherent procedural limitations as discussed above, in addition to the difficulty in estimating catchment rainfall for medium to large catchments, as well as the relatively few catchment response time studies conducted in medium to large catchments internationally, emphasise the need for the development of a new approach to estimate catchment response times for medium to large catchments using only observed streamflow data.

The aim or objective of this study is to develop a new and consistent approach to derive catchment response times in medium to large catchments (20 km<sup>2</sup> to 35,000 km<sup>2</sup>), expressed as the time to peak ( $T_{px}$ ), using only observed streamflow data. For us to develop relationships to estimate catchment response time parameters in ungauged catchments, it is necessary to derive "observed" catchment response time parameters from gauged catchments. Hence, the focus is on the direct estimation of catchment response time parameters using observed streamflow data in gauged catchments, whereas empirical equations are calibrated against these direct estimates by considering various physical catchment characteristics to

estimate the catchment response time in ungauged medium to large catchments. Given the variability in mainly rainfall over a catchment, it is recognised that catchment response times between observed events will differ, but a “representative” catchment response time is required for single-event design flood estimation methods. The methodology proposed in this study recognises the variability in catchment response times between events and uses three approaches to estimate a representative, average catchment  $T_{Px}$  value by investigating the relationship between time parameters and the relevance of conceptualised triangular-shaped direct runoff hydrograph approximations and linear catchment response functions in four climatologically different regions of SA.

## 2 | STUDY ASSUMPTIONS

This study is based on the following assumptions:

- The conceptual  $T_C$  equals  $T_p$ . The conceptual  $T_C$  is normally defined as the time required for the entire catchment to contribute runoff at the catchment outlet, that is, the time taken to flow to the outlet from the furthest point in the catchment.  $T_p$  is defined as the time interval between the start of effective rainfall and the peak discharge of a single-peaked hydrograph (Kirpich, 1940; McCuen et al., 1984; McCuen, 2005; USDA NRCS, 2010; SANRAL, 2013). However, this definition of  $T_p$  is also regarded as the conceptual definition of  $T_C$  (McCuen

et al., 1984; USDA SCS, 1985; Linsley et al., 1988; Seybert, 2006) and Gericke and Smithers (2014) also showed that  $T_C \approx T_p$ .

- $T_p$  equals the total net rise of a multi-peaked hydrograph. At medium to large catchment scales, Du Plessis (1984) demonstrated that  $T_{Pxi}$ , as shown in Figure 1 and expressed in Equation 1, is equal to the duration of the total net rise of a multi-peaked hydrograph.

$$T_{Pxi} = \sum_{j=1}^N t_j, \quad (1)$$

where  $T_{Pxi}$  is the observed time to peak, which equals the conceptual  $T_C$  for individual flood events (h),  $t_j$  is the duration of the total net rise (excluding the in-between recession limbs) of a multi-peaked hydrograph (h), and  $N$  is the sample size.

The approximation of  $T_C \approx T_p$  as proposed by Gericke and Smithers (2014) forms the basis for the new approach developed in this study to derive  $T_{Px}$  and is based on the definition that the volume of effective rainfall equals the volume of direct runoff when a hydrograph is separated into direct runoff and baseflow. The separation point on the hydrograph is regarded as the start of direct runoff, which coincides with the onset of effective rainfall. In other words, the required extensive convolution process normally required to estimate  $T_p$  is eliminated, because  $T_{Px}$  is derived directly from the observed streamflow data without the need for rainfall data.

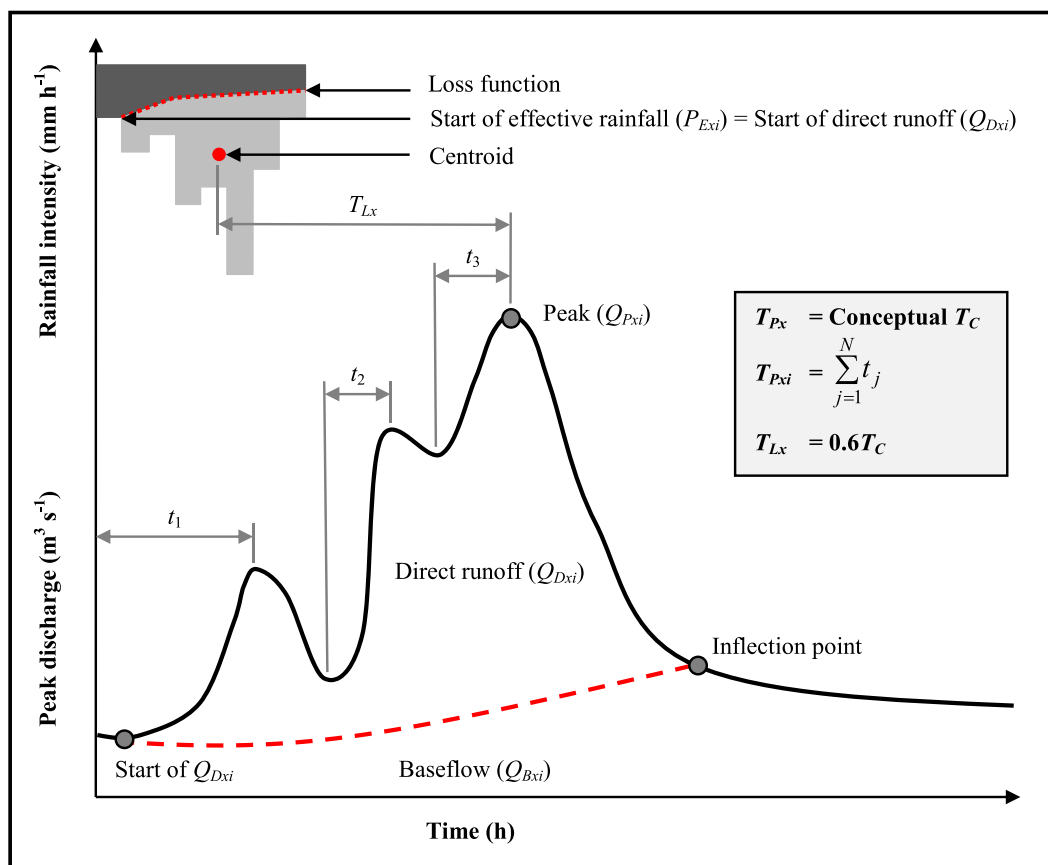
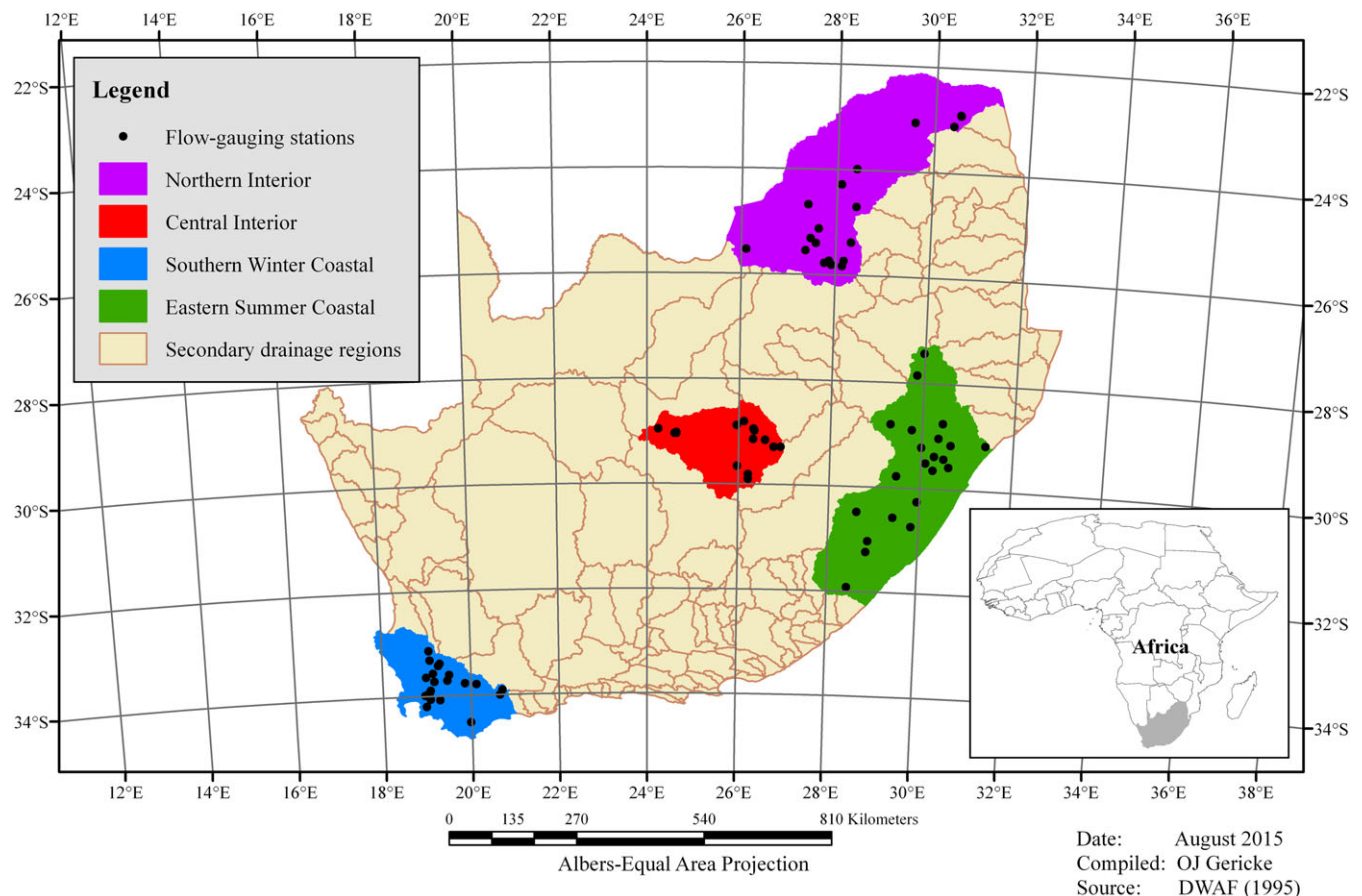


FIGURE 1 Schematic illustrative of the conceptual  $T_C$  and  $T_{Px}$  relationship for multi-peaked hydrographs (after Gericke and Smithers, 2015)

### 3 | STUDY AREA

SA, which is located on the most southern tip of Africa (Figure 2), is demarcated into 22 primary drainage regions, that is, A to X (Midgley et al., 1994), which are further delineated into 148 secondary drainage regions, that is, A1, A2, to X4. In this study, 74 study catchments were selected in four climatologically different regions (Figure 2), summarised as follows:

- Northern Interior (NI).** Seventeen catchments with areas ranging from 61 to 23,852 km<sup>2</sup> and located in the A2, A3, A5 to A7, and A9 secondary drainage regions (Midgley et al., 1994), were selected in this climatological region, which is predominantly characterised by summer rainfall. The mean annual precipitation (MAP) ranges from 348 to 2,031 mm (Lynch, 2004) and rainfall is characterised as highly variable. The topography is moderately steep with elevations varying from 544 to 1,763 m and with average catchment slopes between 3.5% and 21.6% (USGS, 2002). Eight hundred and twenty-three observed flood events from 1904 to 2013 were extracted and included in the final analysis.
- Central Interior (CI).** Sixteen catchments with areas ranging from 39 to 33,278 km<sup>2</sup> and extending across the C5 secondary drainage region (Midgley et al., 1994) were selected in this climatological region, which is predominantly characterised by convective rainfall during the summer months. The MAP ranges
- Southern Winter Coastal (SWC).** Nineteen catchments with areas ranging from 22 to 2,878 km<sup>2</sup> and located in the G1, G2, G4, H1 to H4, and H6 to H7 secondary drainage regions (Midgley et al., 1994) were selected in this climatological region. The MAP ranges from 192 to 1,834 mm (Lynch, 2004), and the winter rainfall is classified as either orographic and/or frontal rainfall. The topography is very steep with elevations varying from 86 to 2,060 m and with average catchment slopes ranging between 2.8% and 51.9% (USGS, 2002). One thousand two hundred and ninety-one observed flood events from 1920 to 2013 were extracted and included in the final analysis.
- Eastern Summer Coastal (ESC).** Twenty-two catchments with areas ranging from 129 to 28,893 km<sup>2</sup> and located in the T1, T3 to T5, U2, U4, V1 to V3, and V5 to V6 secondary drainage regions (Midgley et al., 1994) were selected in this climatological region, which is predominantly characterised by all year and/or summer rainfall. The MAP ranges from 616 to 1,564 mm (Lynch, 2004). The topography is very steep with elevations varying from 31 to 3,149 m and with average catchment slopes ranging between 11% and 41.4% (USGS, 2002). One thousand and ninety observed



**FIGURE 2** Location of the four regions

flood events from 1927 to 2013 were extracted and included in the final analysis.

## 4 | METHODOLOGY

The methodology adopted in the four climatological regions enabled the investigation and analyses of: (a) the variability in individual time to peak ( $T_{Pxi}$ ) values derived from individual flood events and the use of these to estimate a representative catchment  $T_{Px}$  value, (b) the use of triangular-shaped direct runoff hydrograph approximations to represent individual  $T_{Pxi}$  values by incorporating variable hydrograph shape parameters, which reflect the actual percentage of direct runoff under the rising limb of each individual hydrograph, (c) the relationship between paired individual observed peak discharge ( $Q_{Pxi}$ ) and direct runoff volume ( $Q_{Dxi}$ ) values by assuming a linear catchment response function to estimate the catchment  $T_{Px}$  value, and (d) the affect that key climatological and geomorphological catchment characteristics have on the overall catchment response time variability.

The station numbers of the Department of Water and Sanitation (DWS) flow-gauging stations located at the outlet of each catchment are used as the catchment descriptors for easy reference in all the tables and figures.

### 4.1 | Establishment of flood database

A flood database was established by evaluating, preparing, and extracting primary streamflow data for the period up to 2013 from the DWS streamflow database for 74 continuous flow-gauging stations present in the four regions. The screening criteria (a) to (d) used to select the stations for analyses in this study include the following:

- a. Stations common to previous flood studies. All the flow-gaugings stations used by HRU (1972), Hiemstra and Francis (1979), Alexander (2002), Gørgens (2007) and Gørgens et al. (2007) were considered, resulting in 64 flow-gauging stations meeting this criteria.
- b. Record length. Only streamflow records of longer than 20 years were considered; as a result, six of the 74 flow-gauging stations did not meet the criteria. However, three of the latter six flow-gauging stations met the criteria as stipulated in (a) and (c) hence they are included for further analysis. The remaining three stations only met the criteria as stipulated in (c).
- c. Catchment area. In addition to above-listed criteria, the catchment areas of the selected flow-gauging stations should cover the range of catchment areas present in the different regions.
- d. High flows and discharge rating table. Overall, 93% of the flood hydrographs analysed in the 74 catchments were based on standard DWS discharge rating tables, that is, no extrapolation procedure was required. However, in cases where the observed flood levels exceeded the maximum rated flood level ( $H$ ), the rating curve was extrapolated up to bankfull flow conditions using third-order polynomial regression analysis. High flow extensions above bankfull flow conditions were only considered in cases

where the existing discharge rating curve included floodplain flow on the full width of the floodplain. In essence, the individual stage extrapolations ( $H_E$ ), whether for bankfull or above bankfull flow conditions, were limited to a maximum of 20%, that is,  $H_E \leq 1.2 H$ . In the case of above bankfull flow conditions, the relevance of the general extension procedure described above was tested and compared by applying the slope-area method (Ramsbottom & Whitlow, 2003) at some of flow-gauging sites, where surveyed cross-section data were available. In addition to the above-mentioned 20% limit, the hydrograph shape, especially the peakedness as a result of a steep rising limb in relation to the hydrograph base length, and the relationship between individual  $Q_{Pxi}$  and  $Q_{Dxi}$  pair values were used as additional criteria to justify the individual  $H_E$  extrapolations  $\leq 1.2 H$ . Typically, in such an event, the additional volume of direct runoff ( $Q_{DE}$ ) due to the extrapolation was limited to 5%, that is,  $Q_{DE} \leq 0.05 Q_{Dxi}$ . Hence, the error made by using larger direct runoff volumes will have little impact on the sample statistics of the total flood volume. This approach is further justified by taking the total sample size of the analysed flood hydrographs into consideration and given that the primary focus of this study is on the time when the peak discharge occurs, and not on the discharge value.

The details of the 74 flow-gauging stations selected for inclusion in the flood database are listed in Table 1. The average data record length of all the flow-gauging stations listed in Table 1 is 52 years.

### 4.2 | Extraction of flood hydrographs

The next stage involved the identification and extraction of complete flood hydrographs (e.g., peak, volume, and duration) from the primary flow data sets. The Flood Hydrograph Extraction Software developed by Gørgens et al. (2007) was used to assist in identifying and extracting complete flood hydrographs. A Hydrograph Analysis Tool (HAT) was also developed in Microsoft Excel to analyse the large number of extracted flood hydrographs. The use of HAT not only reduced the repetitive processing time of hydrograph analysis and baseflow separation, but it also ensured that an objective and consistent approach was implemented. The following flood hydrograph extraction criteria were used to extract the flood hydrographs:

- a. Truncation levels. Only flood events larger than the smallest annual maximum flood event on record were extracted. Consequently, all minor events were excluded, while all the flood events retained were characterised as multiple events being selected in a specific hydrological year. This approach resulted in a partial duration series of independent flood peaks above a certain level.
- b. Start or end time of flood hydrographs. Flood peaks and flood volumes for the same event were obtained by extracting complete hydrographs. Initially, a large number of streamflow data points prior the start of a hydrograph were identified by physical inspection, where the streamflow changes from nearly constant or declining values to rapidly increasing values, were included in order to identify the potential start of direct runoff. Thereafter, it was acknowledged that, by definition, the volume of effective

**TABLE 1** Information of the 74 flow-gauging stations as included in the flood database

Catchment descriptor	Area (km <sup>2</sup> )	HRU (1972)	Hiemstra and Francis (1979)	Alexander (2002)	Görgens (2007) and Görgens et al. (2007)	Record length		
						Start	End	Years
<b>Northern Interior</b>								
A2H005	774			X		1904	1950	46
A2H006	1,030	X		X	X	1905	2013	108
A2H007	145			X		1908	1951	43
A2H012	2,555		X	X	X	1922	2013	91
A2H013	1,161	X		X	X	1922	2013	91
A2H015	23,852		X			1927	1941	14
A2H017	1,082		X			1927	1937	10
A2H019	6,120				X	1951	2013	62
A2H020	4,546	X				1951	1971	20
A2H021	7,482				X	1955	2013	58
A3H001	1,175	X	X	X		1906	1939	33
A5H004	636			X	X	1955	2013	58
A6H006	180			X	X	1949	2013	64
A7H003	6,700			X		1947	1995	48
A9H001	914	X				1912	2006	94
A9H002	103	X				1931	2000	69
A9H003	61	X				1931	2013	72
<b>Central Interior</b>								
C5H003	1,641	X				1918	2013	95
C5H006	676					1922	1926	4
C5H007	346	X	X	X		1923	2013	90
C5H008	598			X		1931	1986	55
C5H009	189					1931	1986	55
C5H012	2,366	X	X	X		1936	2013	77
C5H014	31,283					1938	2013	75
C5H015	5,939		X	X		1949	1983	34
C5H016	33,278					1953	1999	46
C5H018	17,361					1960	1999	39
C5H022	39					1980	2013	33
C5H023	185					1983	2008	25
C5H035	17,359					1989	2013	24
C5H039	6,331					1970	2013	43
C5H053	4,569					1999	2013	14
C5H054	687					1995	2013	18
<b>Southern Winter Coastal</b>								
G1H002	186	X	X			1920	1970	50
G1H003	47	X		X		1949	2013	64
G1H004	69	X		X	X	1949	2007	58
G1H007	724	X		X		1951	1977	26
G1H008	394	X		X	X	1954	2013	59
G2H008	22	X		X		1947	1995	48
G4H005	146			X	X	1957	2013	56
H1H003	656	X		X		1923	2013	90
H1H006	753		X		X	1950	2013	63
H1H007	80	X	X	X	X	1950	2013	63
H1H018	109		X		X	1969	2013	44
H2H003	743	X		X	X	1950	1986	36
H3H001	594			X		1925	1948	23
H4H005	29			X	X	1950	1981	31

(Continues)

TABLE 1 (Continued)

Catchment descriptor	Area (km <sup>2</sup> )	HRU (1972)	Hiemstra and Francis (1979)	Alexander (2002)	Görgens (2007) and Görgens et al. (2007)	Record length		
						Start	End	Years
H4H006	2,878			X	X	1950	1990	40
H6H003	500			X		1932	1974	42
H6H008	39			X		1964	1992	28
H7H003	458	X				1949	1992	43
H7H004	28	X	X	X	X	1951	2013	62
<b>Eastern Summer Coastal</b>								
T1H004	4,923			X	X	1956	2007	51
T3H002	2,102	X	X	X		1949	2013	64
T3H004	1,026	X		X		1947	2013	66
T3H005	2,565	X			X	1951	2013	62
T3H006	4,282				X	1951	2013	62
T4H001	723	X		X	X	1951	2013	62
T5H001	3,639	X		X		1931	1979	48
T5H004	537	X		X		1949	2013	64
U2H005	2,523			X	X	1950	2013	63
U2H006	338				X	1954	2013	59
U2H011	176				X	1957	2013	56
U2H012	431	X			X	1960	2013	53
U2H013	296	X				1960	2013	53
U4H002	317			X		1949	2013	64
V1H004	446	X				1962	1975	13
V1H009	195	X			X	1954	2013	59
V2H001	1,951	X		X		1931	1976	45
V2H002	945	X		X	X	1950	2013	63
V3H005	677			X	X	1947	1993	46
V3H007	128				X	1948	2013	65
V5H002	28,893			X	X	1956	2013	57
V6H002	12,854			X		1927	2013	86

X = Flow-gauging stations used in previous flood studies.

rainfall is equal to the volume of direct runoff. Therefore, when separating a hydrograph into direct runoff and baseflow using a recursive filtering method, the separation point could be regarded as the start of direct runoff, which coincides with the onset of effective rainfall. Similarly, the end of a flood event, which is when the direct runoff has subsided to only baseflow and which is not directly related to the causative rainfall for that event, was also determined by using recursive filtering methods.

Five thousand six hundred and twenty-five complete flood hydrographs met the extraction criteria as detailed above in Steps (a) to (b) and were considered for further analysis. Due to the nature of the extracted flood hydrographs, it is important to note that the HAT software tool could not automatically deal with all variations in flood hydrographs; hence, a measure of user intervention was required, especially when  $T_{Pxi}$  was determined for multi-peaked hydrographs. The extracted flood hydrographs obtained using the Flood Hydrograph Extraction Software (Görgens et al., 2007) are the input to HAT, and the output includes the following: (a) start or end date or time of flood hydrograph, (b)  $Q_{Pxi}$  (m<sup>3</sup> s<sup>-1</sup>), (c) total volume of runoff ( $Q_{Txi}$ , m<sup>3</sup>), (d)  $Q_{Dxi}$  (m<sup>3</sup>), (e) volume of baseflow ( $Q_{Bxi}$ , m<sup>3</sup>), (f) baseflow index (BFI),

(g) depth of effective rainfall ( $P_{Exi}$ , mm) based on the assumption that the volume of direct runoff equals the volume of effective rainfall and that the total catchment area is contributing to runoff, (h)  $T_{Pxi}$  (h), computed using Equation 1, and (i) a summary of results.

### 4.3 | Analyses of flood hydrographs

A number of methods (e.g., graphical, recursive digital filters, frequency-duration, and recession analysis) have been proposed in the literature to separate direct runoff and baseflow (Nathan & McMahon, 1990; Arnold et al., 1995; Smakhtin, 2001; McCuen, 2005). Recursive digital filtering methods are the most frequently used approaches to separate direct runoff and baseflow, despite having no true physical or hydrological basis, but it is objective and reproducible for continuous baseflow separation (Arnold et al., 1995). According to Smakhtin (2001), the most well-known and widely used recursive filtering methods are those developed by Nathan and McMahon (1990) and Chapman (1999). Smakhtin and Watkins (1997) also adopted the methodology as proposed by Nathan and McMahon (1990) with some modifications in a national-scale study in SA. Hence, based on these recommendations and the need for consistency and reproducibility,

the above-mentioned methods were considered in this study. Equation 2 as proposed by Nathan and McMahon (1990) was implemented by Smakhtin and Watkins (1997), and Chapman (1999) used Equation 3.

$$Q_{Dxi} = \alpha Q_{Dx(i-1)} + \beta(1 + \alpha)(Q_{Tx(i)} - Q_{Tx(i-1)}), \quad (2)$$

$$Q_{Dxi} = \left(\frac{3\alpha-1}{3-\alpha}\right)Q_{Dx(i-1)} + \frac{2}{(3-\alpha)}(Q_{Tx(i)} - Q_{Tx(i-1)}), \quad (3)$$

where  $Q_{Dxi}$  is the filtered direct runoff at time step  $i$ , which is subject to  $Q_{Dx} \geq 0$  for time  $i$  ( $\text{m}^3 \text{s}^{-1}$ ),  $\alpha$  and  $\beta$  are the filter parameters, and  $Q_{Tx(i)}$  is the total streamflow (direct runoff plus baseflow) at time step  $i$  ( $\text{m}^3 \text{s}^{-1}$ ).

Smakhtin and Watkins (1997) established that a fixed  $\alpha$ -parameter of 0.995 is suitable for most catchments in SA, although in some catchments,  $\alpha$ -parameter values of 0.997 proved to be more appropriate. Hughes et al. (2003) also highlighted that a fixed  $\beta$ -parameter value of 0.5 could be used with daily time-step data, because there is more than enough flexibility in the setting of the  $\alpha$ -parameter to achieve an acceptable result. Consequently, a fixed  $\alpha$ -parameter equal to 0.995 and  $\beta$  parameter equal to 0.5 was used in all the catchments in this study. However, in some of the catchments with data sets having sub-daily data with time intervals as short as 12 min (especially after the year 2000), the  $\alpha$ -parameter of 0.995 resulted in a too high proportion of baseflow relative to total flow. In such cases, the average baseflow index of the pre-2000 data years was used to adjust the baseflow volumes accordingly. Comparable or similar results were obtained by increasing the  $\alpha$ -parameter value to 0.997.

The flood hydrographs analysed in each catchment were then subjected to a final screening process to ensure that all the flood

hydrographs are independent and that the  $T_{Pxi}$  estimates are consistent. The final screening process included the following:

- The analysed flood hydrographs were visually inspected and initially selected based on hydrograph shape, for example, number and nature of multiple peaks and smoothness of recession limbs.
- The remaining flood hydrographs, as selected in Step (a), were then ranked in terms of  $Q_{Pxi}$  in a descending order of magnitude in order to check for inconsistencies between  $Q_{Pxi}$ ,  $Q_{Dxi}$ , and  $T_{Pxi}$  values. The "inconsistencies" refer to the fact that the direct  $T_{Pxi}$  estimations from observed streamflow data could vary significantly and acknowledge that the largest  $Q_{Pxi}$  and  $T_{Pxi}$  values are associated with the likelihood of the entire catchment receiving rainfall, and smaller  $T_{Pxi}$  values could be expected when effective rainfall of high average intensity does not cover the entire catchment.
- Thereafter, a triangular approximation of each direct runoff hydrograph based on Equation 4 and illustrated in Figure 3 was used to estimate individual  $T_{Pxi}$  values for the purpose of comparison with the values computed using Equation 1. Equation 4 incorporates a variable hydrograph shape parameter ( $K$ ) to present the actual direct runoff volumes under the rising limb ( $Q_{DRi}$ ) of each hydrograph as shown in Figure 3. The  $K$  values are estimated using Equation 4a. Solving for the base length of the triangle, if one unit of time  $T_{Pxi}$  equals the variable  $Q_{DRi}$  percent of volume (fraction), then the hydrograph base length equals  $1/Q_{DRi}$  units of time. Therefore, the associated recession time ( $T_{Rxi}$ ) and

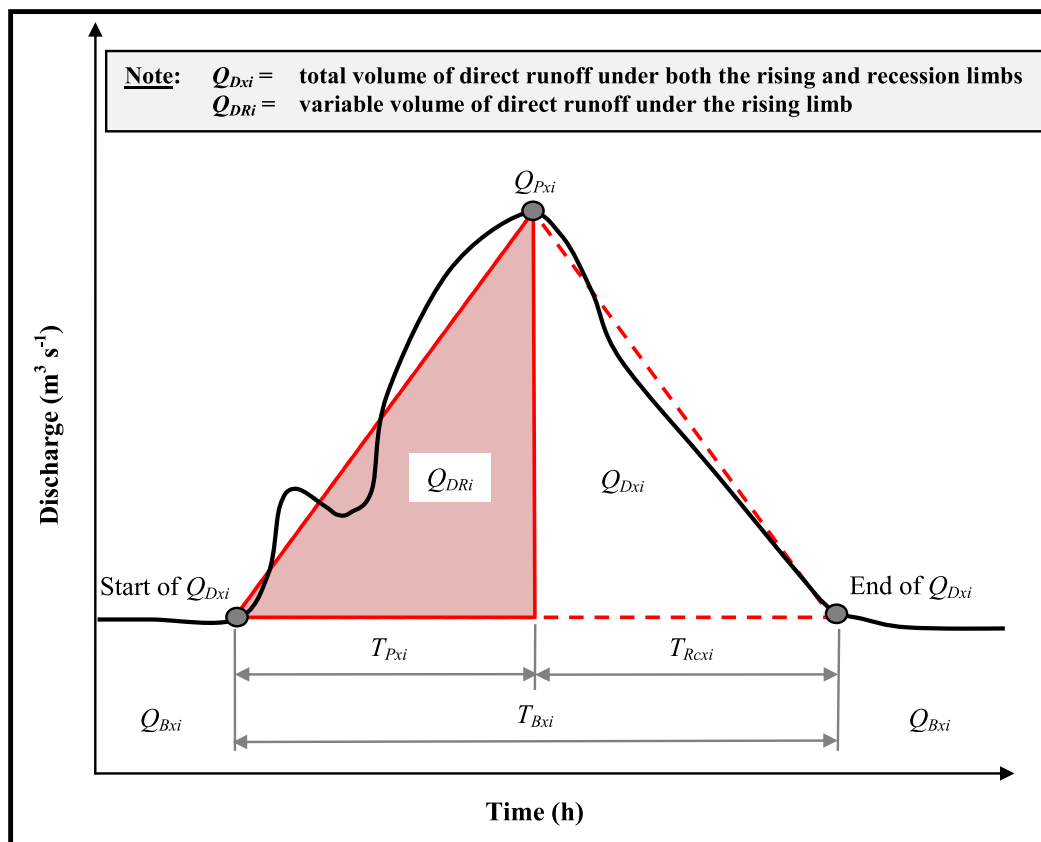


FIGURE 3 Schematic illustrative of the triangular-shaped direct runoff hydrograph approximation (Equation 4)

triangular hydrograph base length ( $T_{Bxi}$ ) could be estimated using Equations 4b and 4c, respectively.

- d. The relationship between  $Q_{Pxi}$  and  $Q_{Dxi}$  was then investigated using the slope of the linear regression between corresponding  $Q_{Pxi}$  and  $Q_{Dxi}$  values of each flood event in individual catchments to provide an estimation of the catchment  $T_{Px}$  value using Equation 5. It is important to note that the use of Equation 5 provides only a single average catchment  $T_{Px}$  value as required for deterministic design flood estimation. The slope of the assumed linear catchment response function in Equation 5 depicts the rate of change between corresponding  $Q_{Pxi}$  and  $Q_{Dxi}$  values along the linear regression and equals the average catchment  $T_{Px}$  value. As a result, the slope of the linear regression is also expressed in units of time (h). The derivation of the linear catchment response function (Equation 5) is included in Appendix A.
- e. The final set of flood hydrographs in a specific catchment was regarded as acceptable and free of any outliers when the averages of the individual  $T_{Pxi}$  values using both Equations 1 and 4 were similar to the catchment  $T_{Px}$  value based on Equation 5. Equation 5 is regarded as a very useful "representative value" to ensure that the averages of individual  $T_{Pxi}$  values (using either Equation 1 or 4) provide a good indication of the catchment conditions and sample mean.

$$T_{Pxi} = K \left[ \frac{Q_{Dxi}}{3600xQ_{Pxi}} \right], \quad (4)$$

$$K = 2 \left[ \frac{Q_{DRI}}{Q_{Dxi}} \right], \quad (4a)$$

$$T_{Rcxi} = T_{Pxi} \left[ \left( \frac{Q_{Dxi}}{Q_{DRI}} \right) - 1 \right], \quad (4b)$$

$$T_{Bxi} = T_{Pxi} + T_{Rcxi}, \quad (4c)$$

$$T_{Px} = \frac{1}{3600x} \left[ \frac{\sum_{i=1}^N (Q_{Pxi} - \overline{Q_{Px}})(Q_{Dxi} - \overline{Q_{Dx}})}{\sum_{i=1}^N (Q_{Pxi} - \overline{Q_{Px}})^2} \right], \quad (5)$$

where  $T_{Bxi}$  is the triangular hydrograph base length for individual flood events (h),  $T_{Px}$  is the "average" catchment time to peak based on a linear catchment response function (h),  $T_{Pxi}$  is the triangular approximated time to peak for individual flood events (h),  $T_{Rcxi}$  is the recession time for individual flood events (h),  $Q_{Dxi}$  is the volume of direct runoff for individual flood events ( $m^3$ ),  $Q_{DRI}$  is volume of direct runoff under the rising limb for individual flood events ( $m^3$ ),  $\overline{Q_{Dx}}$  is the mean of  $Q_{Dxi}$  ( $m^3$ ),  $Q_{Pxi}$  is the observed peak discharge for individual flood events ( $m^3 s^{-1}$ ),  $\overline{Q_{Px}}$  is the mean of  $Q_{Pxi}$  ( $m^3 s^{-1}$ ),  $K$  is the hydrograph shape parameter,  $N$  is the sample size, and  $x$  is a variable proportionality ratio (default  $x = 1$ ), which depends on the catchment response time parameter under consideration.

It is important to note that the variable proportionality ratio ( $x$ ) is included in Equation 5 to increase the flexibility and use thereof, that is, with  $x = 1$ , either  $T_{Px}$  or  $T_{Cx}$  could be estimated by acknowledging the approximation of  $T_C \approx T_P$  (Gericke and Smithers, 2014) and with

$x = 1.667$ ,  $T_L$  could be estimated by assuming that  $T_L = 0.6T_C$ , which is the time from the centroid of effective rainfall to the time of peak discharge (McCuen, 2009).

Tables 2A to 2D provide a summary of the average catchment conditions based on the individual analysis using above-mentioned procedures and the averages of Equations 1 and 4, as well as the catchment  $T_{Px}$  values computed using Equation 5 in each catchment under consideration.

## 5 | RESULTS

The 5,625 analysed flood hydrographs were characterised by a high variability between individual  $T_{Pxi}$  responses (Equation 1) and corresponding  $Q_{Pxi}$  values. Such a high variability of event-based catchment responses could typically result in misleading average catchment values, which are not representative of the true catchment processes, and confirmed the need for the final screening process, as detailed in the Methodology. Consequently, the analysed flood hydrographs were reduced to 4,139 after the final screening. Figure 4 shows the regional observed  $Q_{Pxi}$  versus  $T_{Pxi}$  values computed using Equation 1 for all the catchments in each of the four regions.

Despite following the final screening process, the scatter of data in Figure 4 still demonstrates the inherent variability of  $T_{Pxi}$  at a regional level. The high variability between individual  $T_{Pxi}$  (Equation 1) and corresponding  $Q_{Pxi}$  values, as shown in Figure 4, is regarded as being directly related and amplified by the catchment area, especially the relationship between catchments with larger areas and the spatial distribution of catchment rainfall, as characterised by many rainfall events not covering the entire catchment. Apart from catchment area, the catchment shape could also have an influence on the variability of the  $T_{Pxi}$ - $Q_{Pxi}$  values. In elongated elliptically shaped catchments of comparable size in all the regions, the runoff is more evenly distributed over time, thus resulting in higher  $T_{Pxi}$  and lower  $Q_{Pxi}$  values, when compared to that of circular shaped catchments. Topographical variability within a catchment also has a direct influence on catchment response time. However, the developed  $T_{Px}$  approach is mostly to be applied in deterministic design flood estimation methods, which considers only the average catchment slope ( $S$ ) and the average main watercourse slope ( $S_{CH}$ ) conditions. In general, the catchments with steep upper reaches and flat valleys, that is, large differences between  $S$  and  $S_{CH}$ , are characterised by shorter travel times and hence higher  $Q_{Pxi}$  values. The ratios between  $S$  and  $S_{CH}$  are similar in the NI, CI, and SWC regions, that is, the average ratios of the slope descriptors ( $S:S_{CH}$ ) vary between 12 and 20. Generally, the higher average  $S:S_{CH}$  ratio of 32 in the ESC region resulted in lower  $T_{Pxi}$  and corresponding higher  $Q_{Pxi}$  values; hence, topographical variability within a catchment does impact on  $T_{Pxi}$  values.

In using Equation 4 to estimate individual  $T_{Pxi}$  values by incorporating a triangular approximated hydrograph shape parameter, the variability of  $Q_{DRI}$  under the rising limb of individual hydrographs is evident. In Figure 5, a frequency distribution histogram of the  $Q_{DRI}$  values expressed as a percentage of the total direct runoff volume ( $Q_{Dxi}$ ) is shown. Taking into consideration that 5,625 individual flood hydrographs were analysed, a few flood events could be characterised

**TABLE 2A** Summary of average catchment results in the Northern Interior

Catchment (area, km <sup>2</sup> )	Period	Number of events	Average catchment values							
			Q <sub>Tx</sub> (10 <sup>6</sup> m <sup>3</sup> )	Q <sub>Dx</sub> (10 <sup>6</sup> m <sup>3</sup> )	Q <sub>Px</sub> (m <sup>3</sup> s <sup>-1</sup> )	T <sub>Px</sub> (Equation 1)	T <sub>Px</sub> (Equation 4)	T <sub>Px</sub> (Equation 5)	P <sub>Ex</sub> (mm)	BFI
A2H005 (774)	1904/11/16 to 1950/10/01	60	2.1	1.7	14.7	12.8	14.8	14.3	2.2	0.2
A2H006 (1,030)	1905/03/01 to 2013/09/17	100	8.6	6.4	79.8	11.4	11.2	11.2	6.2	0.2
A2H007 (145)	1908/07/01 to 1951/08/01	60	0.8	0.7	40.2	4.0	2.4	4.1	4.6	0.2
A2H012 (2,555)	1922/10/01 to 2013/09/18	70	17.3	11.0	190.9	11.9	10.8	12.4	4.3	0.3
A2H013 (1,161)	1922/10/01 to 2013/09/18	60	6.0	3.9	80.3	8.1	7.6	8.0	3.4	0.3
A2H015 (23,852)	1927/10/01 to 1931/09/41	15	12.6	10.7	85.8	28.0	23.9	28.8	0.4	0.2
A2H017 (1,082)	1927/12/08 to 1937/01/31	18	1.4	1.2	29.6	5.9	5.5	6.2	1.1	0.1
A2H019 (6,120)	1951/02/15 to 2013/08/27	60	42.3	33.5	205.1	25.0	27.4	25.5	5.5	0.2
A2H020 (4,546)	1951/02/01 to 1970/11/23	40	28.3	22.8	250.0	21.5	21.1	24.4	5.0	0.2
A2H021 (7,482)	1955/09/01 to 2013/08/27	30	74.8	49.0	145.3	80.7	80.4	79.6	6.5	0.3
A3H001 (1,175)	1906/09/01 to 1939/09/30	50	1.0	0.8	34.0	3.3	3.1	3.3	0.7	0.1
A5H004 (636)	1955/12/01 to 2013/08/22	30	19.5	10.3	89.6	18.3	17.1	19.0	16.2	0.5
A6H006 (180)	1949/08/01 to 2013/08/22	65	1.9	1.5	21.5	12.7	12.6	12.4	8.3	0.2
A7H003 (6,700)	1947/10/01 to 1995/11/08	40	7.1	5.8	53.6	17.6	20.6	19.9	0.9	0.2
A9H001 (914)	1912/12/12 to 2006/04/27	60	15.8	10.8	58.8	32.5	30.7	30.2	11.8	0.3
A9H002 (103)	1931/09/20 to 2000/02/23	16	6.5	3.9	66.7	7.3	7.2	7.5	38.2	0.3
A9H003 (61)	1931/09/02 to 2013/08/14	49	3.4	1.7	49.3	3.5	3.3	4.3	28.3	0.4

Note. BFI = baseflow index.

**TABLE 2B** Summary of average catchment results in the Central Interior

Catchment (area, km <sup>2</sup> )	Period	Number of events	Average catchment values							
			Q <sub>Tx</sub> (10 <sup>6</sup> m <sup>3</sup> )	Q <sub>Dx</sub> (10 <sup>6</sup> m <sup>3</sup> )	Q <sub>Px</sub> (m <sup>3</sup> s <sup>-1</sup> )	T <sub>Px</sub> (Equation 1)	T <sub>Px</sub> (Equation 4)	T <sub>Px</sub> (Equation 5)	P <sub>Ex</sub> (mm)	BFI
C5H003 (1,641)	1918/07/01 to 2013/06/26	101	2.1	1.7	32.8	9.1	11.0	11.1	1.0	0.2
C5H006 (676)	1922/11/13 to 1926/12/31	14	1.4	1.3	36.0	7.3	6.4	8.2	1.9	0.1
C5H007 (346)	1923/10/01 to 2013/08/06	91	1.2	1.0	28.0	6.4	7.3	7.2	2.9	0.1
C5H008 (598)	1931/04/01 to 1986/04/01	112	2.2	2.0	44.7	8.0	8.6	10.5	3.3	0.1
C5H009 (189)	1931/03/01 to 1986/05/11	13	1.0	0.8	14.3	11.8	13.0	12.7	4.5	0.1
C5H012 (2,366)	1936/04/01 to 2013/02/13	68	3.3	2.3	41.5	11.8	11.0	11.9	1.0	0.3
C5H014 (31,283)	1938/10/17 to 2013/07/25	28	46.7	36.5	168.3	46.2	57.0	56.6	1.2	0.2
C5H015 (5,939)	1949/01/01 to 1983/11/22	90	23.3	21.0	203.1	26.7	24.8	25.0	3.5	0.1
C5H016 (33,278)	1953/02/01 to 1999/03/10	40	31.0	27.0	105.6	65.9	54.7	65.6	0.8	0.1
C5H018 (17,361)	1960/02/23 to 1999/03/15	50	22.8	19.7	105.0	32.3	37.8	39.0	1.1	0.1
C5H022 (39)	1980/10/14 to 2013/10/24	69	0.4	0.3	11.5	5.3	5.5	6.1	8.0	0.2
C5H023 (185)	1983/06/04 to 2008/03/22	58	0.8	0.6	15.6	6.8	7.7	9.8	3.3	0.2
C5H035 (17,359)	1989/08/03 to 2013/07/23	20	10.8	9.1	58.9	32.3	41.8	40.7	0.5	0.2
C5H039 (6,331)	1970/11/24 to 2013/08/08	56	34.0	29.2	136.2	44.1	54.7	55.7	4.6	0.1
C5H053 (4,569)	1999/11/29 to 2013/08/08	65	8.3	5.7	93.1	17.3	15.3	16.4	1.3	0.3
C5H054 (687)	1995/10/18 to 2013/08/08	60	1.3	0.8	21.3	8.8	8.2	8.7	1.2	0.4

Note. BFI = baseflow index.

by either low (0.4%) or high (98.1%)  $Q_{DRI}$  values. However, more than 60% of the  $Q_{DRI}$  values are within the 20 ~ 40% range. At a catchment level, the values of  $Q_{DRI}$  ranged on average from 29.3% to 36.3% in the four regions. The latter  $Q_{DRI}$  percentages are in close agreement with the 37.5% of the volume under the rising limb generally associated with the conceptual curvilinear unit hydrograph theory (USDA NRCS, 2010).

A scatter plot of the  $T_{Pxi}$  values computed using of Equations 1 and 4 for all the catchments under consideration is shown in Figure 6.

In comparing Equations 1 and 4 at a catchment level in the four regions, the  $r^2$  value of 0.69 (based on the 4,139 flood hydrographs) confirmed not only the relatively high degree of association but also the usefulness of Equation 4. Taking into consideration the influence catchment area has on response times, the degree of association between these individual  $T_{Pxi}$  values could decrease with an increase in catchment area; however, the ultimate goal is to estimate the average catchment  $T_{Px}$  by considering the sample mean of the individual responses based on Equations 1 and 4.

**TABLE 2C** Summary of average catchment results in the SWC region

Catchment (area, km <sup>2</sup> )	Period	Number of events	Average catchment values							
			Q <sub>Tx</sub> (10 <sup>6</sup> m <sup>3</sup> )	Q <sub>Dx</sub> (10 <sup>6</sup> m <sup>3</sup> )	Q <sub>Px</sub> (m <sup>3</sup> s <sup>-1</sup> )	T <sub>Px</sub> (Equation 1)	T <sub>Px</sub> (Equation 4)	T <sub>Px</sub> (Equation 5)	P <sub>Ex</sub> (mm)	BFI
G1H002 (186)	1920/12/01 to 1970/10/05	90	8.1	5.8	123.8	8.7	6.4	6.4	31.1	0.3
G1H003 (47)	1949/03/21 to 2013/08/27	75	1.6	1.2	20.6	8.3	9.1	9.2	24.4	0.2
G1H004 (69)	1949/04/01 to 2007/05/17	77	12.1	9.8	228.9	13.2	10.1	13.3	142.4	0.2
G1H007 (724)	1951/04/02 to 1977/05/31	75	50.4	43.9	238.9	36.0	35.0	37.1	60.7	0.1
G1H008 (394)	1954/05/01 to 2013/07/25	75	12.2	8.5	139.5	11.9	10.0	10.8	21.6	0.3
G2H008 (22)	1947/06/01 to 1995/04/07	106	1.7	1.3	23.7	8.4	8.9	8.9	60.6	0.2
G4H005 (146)	1957/03/11 to 2013/08/29	55	15.8	12.5	79.7	31.4	31.5	32.4	79.2	0.2
H1H003 (656)	1923/02/22 to 2013/07/15	72	15.1	11.6	115.0	21.2	21.0	21.2	17.7	0.2
H1H006 (753)	1950/04/16 to 2013/07/25	90	25.9	18.1	273.6	14.6	15.4	15.1	24.1	0.3
H1H007 (80)	1950/04/10 to 2013/07/25	98	10.5	7.6	196.8	10.3	10.2	10.3	95.0	0.3
H1H018 (109)	1969/02/26 to 2013/07/26	80	15.0	11.0	323.3	11.1	8.3	10.9	100.9	0.3
H2H003 (743)	1950/05/01 to 1986/05/05	45	7.6	5.3	67.9	11.2	12.6	12.8	7.1	0.3
H3H001 (594)	1925/11/01 to 1948/05/01	25	5.6	5.2	97.8	11.9	10.1	12.5	8.8	0.1
H4H005 (29)	1950/04/01 to 1981/12/21	30	0.8	0.6	12.1	8.7	8.6	8.6	20.5	0.2
H4H006 (2,878)	1950/04/19 to 1990/08/06	80	105.7	78.8	453.5	43.9	41.3	44.8	27.4	0.2
H6H003 (500)	1932/10/01 to 1974/11/11	52	16.9	13.1	58.1	31.5	32.1	32.1	26.3	0.2
H6H008 (39)	1964/04/18 to 1992/09/07	60	2.6	1.9	41.2	6.1	6.6	6.7	49.2	0.2
H7H003 (458)	1949/03/15 to 1992/10/01	70	8.3	7.3	74.7	16.0	16.4	16.5	15.9	0.1
H7H004 (28)	1951/05/02 to 2013/06/19	36	1.2	0.8	25.2	7.0	6.6	6.8	29.8	0.3

Note. BFI = baseflow index; SWC = Southern Winter Coastal.

**TABLE 2D** Summary of average catchment results in the ESC region

Catchment (area, km <sup>2</sup> )	Period	Number of events	Average catchment values							
			Q <sub>Tx</sub> (10 <sup>6</sup> m <sup>3</sup> )	Q <sub>Dx</sub> (10 <sup>6</sup> m <sup>3</sup> )	Q <sub>Px</sub> (m <sup>3</sup> s <sup>-1</sup> )	T <sub>Px</sub> (Equation 1)	T <sub>Px</sub> (Equation 4)	T <sub>Px</sub> (Equation 5)	P <sub>Ex</sub> (mm)	BFI
T1H004 (4,923)	1956/06/04 to 2007/04/04	80	42.9	30.7	271.7	30.8	26.6	30.8	6.2	0.4
T3H002 (2,102)	1949/08/01 to 2013/10/16	67	46.2	26.1	203.6	28.5	27.8	28.8	12.4	0.4
T3H004 (1,026)	1947/09/01 to 2013/10/17	38	18.5	10.1	48.2	35.4	36.7	37.2	9.9	0.4
T3H005 (2,565)	1951/09/20 to 2013/10/17	60	97.0	53.6	385.7	32.1	34.9	34.9	18.4	0.4
T3H006 (4,282)	1951/10/16 to 2013/10/17	75	155.8	92.5	552.0	34.1	39.7	39.6	19.7	0.4
T4H001 (723)	1951/09/05 to 2013/10/10	30	37.3	18.7	184.8	24.6	18.7	24.8	25.9	0.5
T5H001 (3,639)	1931/07/19 to 1979/05/07	42	255.3	187.4	444.6	58.5	57.2	57.7	51.5	0.3
T5H004 (537)	1949/07/01 to 2013/10/11	30	46.9	28.6	117.8	22.4	28.9	25.7	48.8	0.4
U2H005 (2,523)	1950/11/01 to 2013/06/07	36	68.3	39.7	151.3	30.3	33.4	32.2	15.7	0.4
U2H006 (338)	1954/01/04 to 2013/07/30	32	25.5	17.3	50.0	38.9	39.7	35.7	50.1	0.3
U2H011 (176)	1957/12/24 to 2013/07/16	40	6.2	3.5	95.6	7.3	6.4	8.8	20.0	0.4
U2H012 (431)	1960/08/11 to 2013/08/13	40	7.6	4.4	72.7	6.2	5.8	6.4	10.3	0.4
U2H013 (296)	1960/08/10 to 2013/05/07	52	11.9	7.1	58.2	9.6	10.3	9.9	23.3	0.4
U4H002 (317)	1949/08/12 to 2013/10/17	30	10.3	6.7	19.9	30.7	37.5	31.1	19.6	0.3
V1H004 (446)	1962/04/08 to 1975/12/10	38	19.0	12.6	119.8	8.6	8.6	8.9	28.3	0.3
V1H009 (195)	1954/01/15 to 2013/11/04	70	4.4	3.8	150.8	5.9	5.0	5.6	19.2	0.2
V2H001 (1,951)	1931/09/14 to 1976/02/08	62	77.1	60.8	191.5	47.1	45.0	47.1	31.2	0.2
V2H002 (945)	1950/06/12 to 2013/10/20	45	62.4	41.6	136.0	57.9	60.6	59.8	43.9	0.3
V3H005 (677)	1947/08/06 to 1993/03/31	60	27.2	19.5	72.6	36.7	38.2	37.2	28.8	0.3
V3H007 (128)	1948/07/01 to 2013/07/16	58	7.0	4.7	51.1	7.3	9.1	9.1	36.3	0.4
V5H002 (28,893)	1956/08/01 to 2013/09/29	75	635.1	385.8	1430.4	62.5	65.2	65.3	13.0	0.4
V6H002 (12,854)	1927/01/01 to 2013/09/13	30	704.7	456.5	1136.6	62.7	69.3	67.7	35.2	0.3

Note. BFI = baseflow index; ESC = Eastern Summer Coastal.

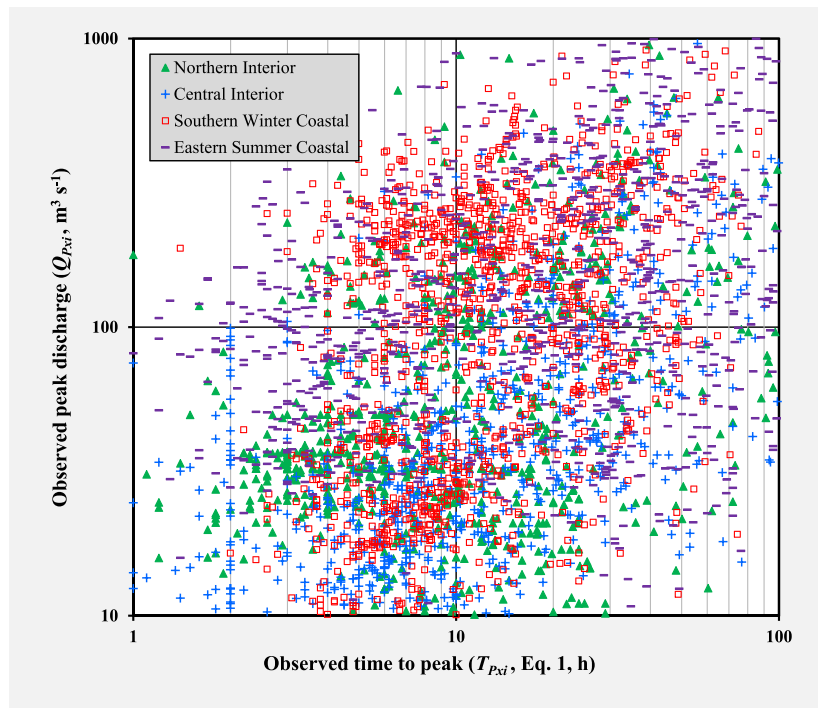


FIGURE 4 Regional  $Q_{Pxi}$  versus  $T_{Pxi}$  values in the four regions

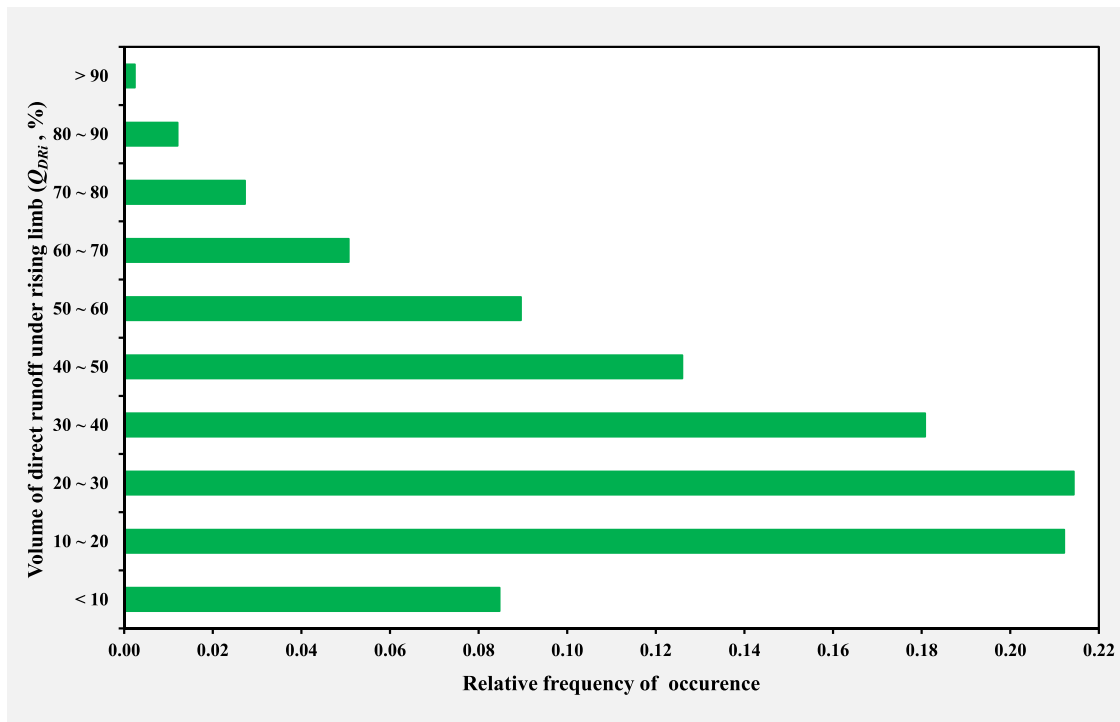
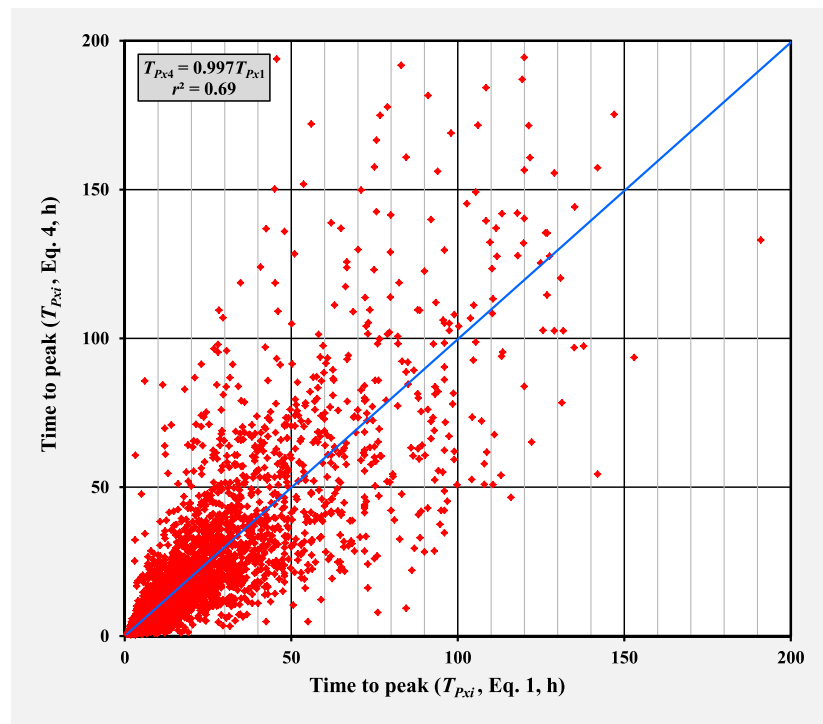


FIGURE 5 Frequency distribution histogram of the  $Q_{DRI}$  values (%) based on the 4,139 analysed flood hydrographs

The regional linear regression plots of the paired  $Q_{Pxi}$  and  $Q_{Dxi}$  values applicable to the four regions are shown in Figure 7. At a regional level, the paired  $Q_{Pxi}$  and  $Q_{Dxi}$  values showed a moderate degree of association with  $r^2$  values between 0.4 and 0.7. In using Equation 5 at a catchment level, the overall degree of association between the corresponding  $Q_{Pxi}$  and  $Q_{Dxi}$  values was much better than at the regional levels shown in Figure 7. Typically, at a catchment level, the  $r^2$  values varied between 0.6 and 0.98.

Fifty percent of the CI catchments could be regarded as “semi-arid,” with the MAP  $\leq 465$  mm; thus, some of the infrequently occurring high intensity rainstorms resulted in more rapid catchment responses, that is, lower  $T_{Pxi}$  values, resulting in the lower  $Q_{Dxi}$  associated with higher  $Q_{Pxi}$  values as shown in Figure 7. Conversely, in the wetter, that is, MAP values between 800 and 1,400 mm, medium to large catchments of the SWC and ESC regions, it could also be argued that the antecedent soil moisture status, the non-uniform distribution



**FIGURE 6** Scatter plot of the  $T_{Pxi}$  pair values computed using Equations 1 and 4

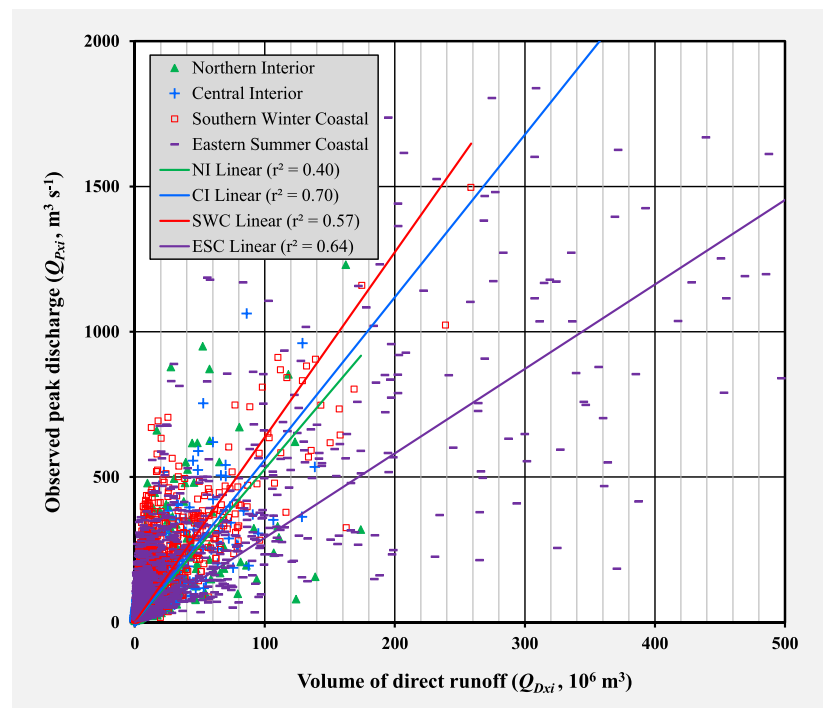


**FIGURE 7** Regional  $Q_{Pxi}$  versus  $Q_{Dxi}$  values in the four regions

of rainfall, and the attenuation of the resulting flood hydrograph as it moves towards the catchment outlet are more influential than the relationship between rainfall intensity and the infiltration rate of the soil. The convective rainfall in the NI and CI is generally of a short duration and high intensity; hence, the lower  $T_{Pxi}$  values are associated with lower  $Q_{Dxi}$  and higher  $Q_{Pxi}$  values in Figure 7. The orographic or frontal rain in the SWC region generally has a low intensity and long duration and is controlled by the local topography; hence the higher  $T_{Pxi}$  and

$Q_{Dxi}$  values in this region. In the ESC region, prolonged high intensity rainfall often resulted in lower  $T_{Pxi}$  and higher  $Q_{Pxi}$  values when compared to similar-sized catchments in the other regions.

Drainage density ( $D_D$ ), that is, the ratio of the total length of water-courses within a catchment to the catchment area, could also have a marked effect on the corresponding  $Q_{Pxi}$  and  $Q_{Dxi}$  values as shown in Figure 7. Typically, Gericke and Smithers (2016) demonstrated that larger proportions of rainfall contribute to direct runoff in the well-

drained ( $D_D > 0.3$ ) catchments, for example, G1H002, G2H008, and H7H004 (SWC region) and U2H006 (ESC region), but the catchment response times are comparatively shorter and hence resulting in steeper flood hydrographs, that is, higher  $Q_{Pxi}$  and lower  $Q_{Dxi}$  values. All the catchments in the NI and CI, with the exception of A2H007, A9H002, A9H003, and C5H003, are characterised by a relatively low drainage density, that is,  $D_D \leq 0.20$  (Gericke and Smithers, 2016). The catchments in the CI, and to a lesser extent the NI catchments, are also generally flatter with some surface depressions, hence the longer catchment response times and lower peak discharges.

In Figures 8a–d, box plots based on Equation 1 are used to highlight the influence of catchment area on the inherent  $T_{Pxi}$  variability. In these figures, the whiskers represent the minimum and maximum values computed using Equation 1, and the boxes, the 25th and 75th percentile values, and the change in box colour represent the median value. The catchment  $T_{Px}$  estimates based on the averages of Equations 1 and 4, as well as Equation 5 is also shown.

The influence of catchment area on the  $T_{Pxi}$  values is clearly evident in Figures 8a–d. Generally, the range of  $T_{Pxi}$  (i.e., the difference between maximum and minimum  $T_{Pxi}$  values for individual flood events) increases with an increase in catchment area. This increased variability with catchment area is probably the result of the spatially non-uniform rainfall in larger catchments. On average, the  $T_{Pxi}$  variability (84.8%) was the lowest in the SWC region with catchment areas ( $A$ )  $\leq 2,878 \text{ km}^2$ , and the  $T_{Pxi}$  variability generally exceeded 90% for  $A > 2,500 \text{ km}^2$  in the NI. However, the spatial rainfall distribution in the CI and ESC region proved to be highly variable despite the catchment area under consideration; hence, the higher  $T_{Pxi}$  variation witnessed in some catchments.

## 6 | DISCUSSION

The primary objective of the study was to develop a new and consistent approach to estimate the catchment  $T_{Px}$  in medium to large

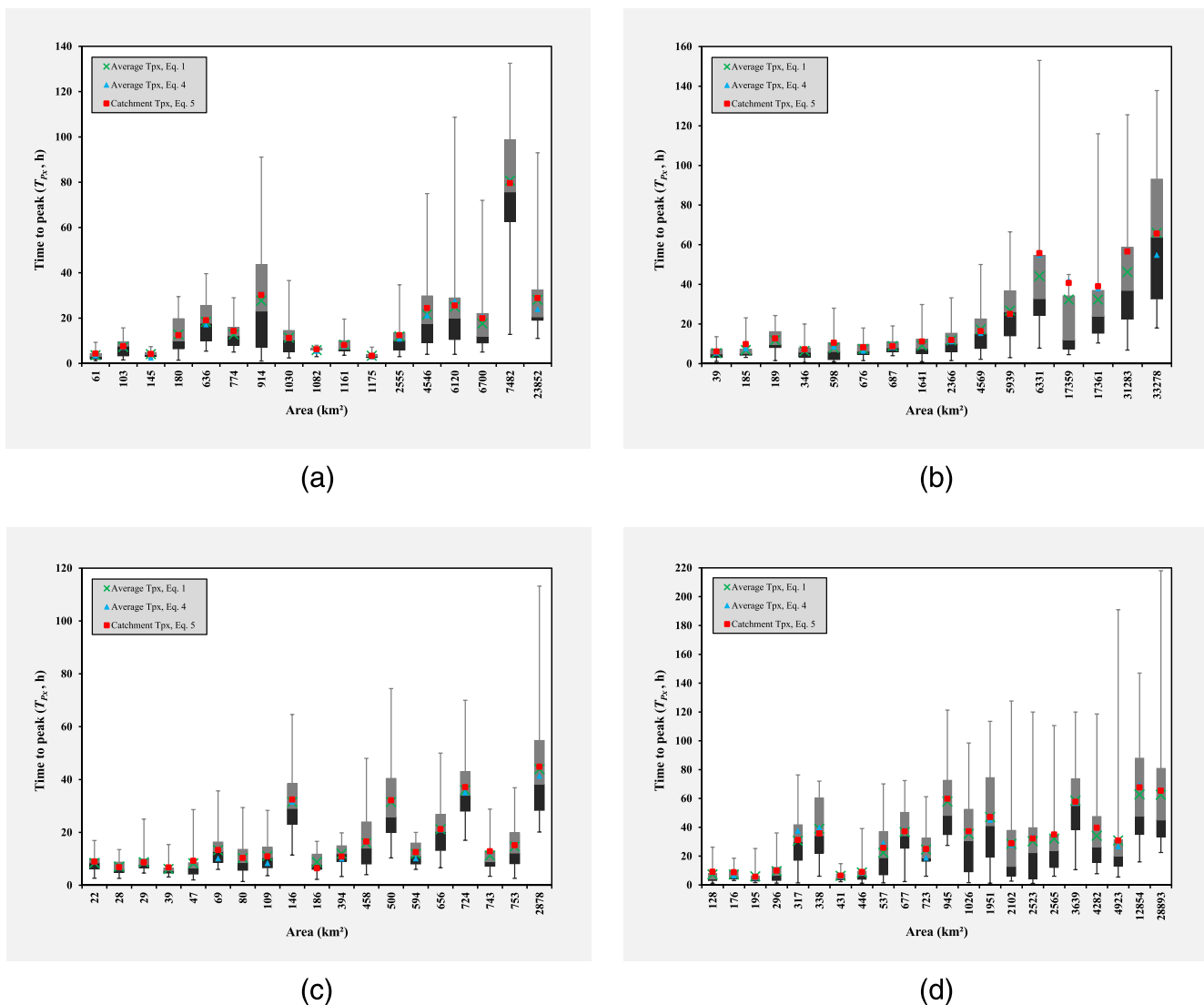


**FIGURE 8** (a–d) Box plots of the  $T_{Pxi}$  values obtained directly from observed streamflow data (Equation 1) and the average  $T_{Px}$  (Equations 1 and 4) and catchment  $T_{Px}$  (Equation 5) estimates for catchments in the (a) Northern Interior, (b) Central Interior, (c) SWC region, and (d) ESC region. CI = Central Interior; ESC = Eastern Summer Coastal; NI = Northern Interior; SWC = Southern Winter Coastal

catchments in SA, derived from using only observed streamflow data. The use of observed streamflow data to estimate catchment response times is necessary, given the lack of appropriate observed rainfall data at these catchment scales, and to provide an alternative new approach to replace the current simplified convolution process, as used in small catchments, to estimate observed catchment response times.

Typically, rainfall and streamflow data are the two primary data sources required when a simplified convolution process is used to estimate observed catchment response times in small catchments. However, as highlighted in the Introduction, such simplified convolution process is neither practical nor applicable in medium to large heterogeneous catchments, where antecedent moisture from previous rainfall events and spatially non-uniform rainfall hyetographs can result in multi-peaked hydrographs. In terms of the availability of rainfall data, not only the number of rainfall stations both internationally and in SA has declined steadily over the past few decades (Pitman, 2011; Lorenz and Kunstmann, 2012) but also the rainfall data are generally widely available only at more aggregated levels, such as daily, and this reflects a paucity of rainfall data at sub-daily timescales, both in the number of rainfall gauges and length of the recorded series. In addition, time variables for an individual event (either from a hyetograph or hydrograph) cannot always be measured directly from autographic records owing to the difficulties in determining the start time, end time, and temporal and spatial distribution of effective rainfall and direct runoff (Schmidt and Schulze, 1984; Gericke and Smithers, 2014). Problems are further compounded by poorly synchronised rainfall and streamflow observations, which contribute to inaccurate estimates of time parameters using a simplified convolution process.

The hydrological literature, unfortunately, often fails to distinguish between the different time parameters or to define the relationship between the time variables used to estimate the time parameters (e.g.,  $T_C$ ,  $T_L$ , and  $T_P$ ). This not only creates confusion but also results in multiple definitions being used to define the same time parameter. McCuen (2009) highlighted that seven different definitions are interchangeably used to define time parameters as obtained from observed rainfall and streamflow data. As a result, time intervals from various points during a storm extracted from a hyetograph to various points on the resultant hydrograph are often misinterpreted as  $T_C$ ,  $T_L$ , and/or  $T_P$ .

As detailed in Gericke and Smithers (2014) and summarised in the Introduction, many methods used internationally and in SA to estimate catchment response times are widely applied outside the regions, where they were derived and well beyond the bounds of the data sets used in the derivation of the equations, that is, equations are derived using data from small catchments and are frequently applied to medium and even to large catchments. This is a consequence of very few studies focusing on the development of catchment response times from medium to large catchments. From the 50 empirical time parameter estimation methods reviewed by Gericke and Smithers (2014), it is clearly evident that the majority of international catchment response time studies are limited to small catchments, with only six studies focusing on larger catchments of up to 5,000 km<sup>2</sup>. It is postulated that the limited number of studies on catchment response times from medium to larger catchments is a consequence of the estimation of catchment

response times from the observed rainfall and streamflow data, as referred to above.

Hence, when using the new proposed approach based on the novel approximation of  $T_C \approx T_P$ , which requires only observed streamflow data, both the extensive convolution process required to estimate time parameters and the need to estimate catchment rainfall data are not required. Although streamflow data are internationally less readily available than rainfall data, the quantity and quality of streamflow data enable the direct estimation of catchment response times at medium to large catchment scales. The results also confirmed that catchment response time in medium to large catchments are much more variable than in small catchments, where a simplified convolution process can be applied. Typically, in medium to large catchments, the largest  $Q_{Pxi}$  and  $T_{Pxi}$  values (cf., Figure 4) are associated with the likelihood of the entire catchment receiving rainfall for the critical storm duration, and smaller  $T_{Pxi}$  values probably occur when the effective rainfall does not cover the entire catchment, for example when a storm is centered near the outlet of a catchment. From the derived data sets, the smaller  $T_{Pxi}$  values, which occurred more frequently, have a large influence on the average value and consequently result in an underestimated representative catchment  $T_{Px}$  value. On the other hand, the longer  $T_{Px}$  values have a lower frequency of occurrence and are reasonable in medium to large catchment scales as the contribution of the whole catchment to peak discharge seldom occurs as a result of the non-uniform spatial and temporal distribution of rainfall in the catchment. In principle, these events should conform to the conceptual definition of  $T_C (\approx T_P)$ , which assumes that  $T_C$  is the time required for runoff generated from effective rainfall, with a uniform spatial and temporal distribution over the whole catchment, to contribute to the peak discharge at the catchment outlet.

In agreement with the findings of Mimikou (1984) and Pegram and Parak (2004), the catchment area was identified as the single most important geomorphological catchment variable as it demonstrates a strong correlation with many flood indices affecting the catchment response time and hence the resulting volume of direct runoff and peak discharge. However, in addition to catchment area and in agreement with other medium to large catchment studies (Johnstone and Cross, 1949; Watt and Chow, 1985; Thomas et al., 2000; Royappen et al., 2002; Sabol, 2008), the combined effect of other geomorphological relatively constant variables for a catchment (e.g., shape, hydraulic lengths, slopes, and drainage density) proved also to be important factors, which impact on catchment response times.

Climatological variables (e.g., MAP and spatial or temporal rainfall distribution) are also regarded as equally important; however, rainfall intensity and distribution are not constant and are dependent on the climatological region in which the catchment is located. Internationally, the inclusion of climatological (rainfall) variables as predictor variables of catchment response time has, to date, been limited to the research conducted by Rao and Delleur (1974), Kadoya and Fukushima (1979), McCuen et al. (1984), Schmidt and Schulze (1984), Papadakis and Kazan (1987), and Loukas and Quick (1996). However, only the research of Kadoya and Fukushima (1979) focused on catchment areas larger than 20 km<sup>2</sup>. Rainfall distribution also has a direct influence on seasonal vegetal cover, which, in turn, could also affect the relationship between corresponding  $Q_{Pxi}$  and  $Q_{Dxi}$  values (cf., Figure 7). For

example, the changes in seasonal and/or annual vegetal cover in the NI and semi-arid CI could introduce more variability in the magnitude, timing, and distribution of the  $T_{Pxi}$ ,  $Q_{Pxi}$ , and  $Q_{Dxi}$  values than in the SWC and ESC regions, where the vegetal cover does not vary significantly between seasons. In agreement with the findings of Royapen et al. (2002), it was also evident that long-term land-use changes do not have a significant impact on catchment response times. In addition,  $T_{Px}$  is directly estimated using Equation 5 from observed streamflow data, which, despite some uncertainties and possible errors in the measurement, are also regarded as being a good indicator of any land-use changes in a catchment over time.

It is also important to note that the approach developed in this study to estimate  $T_{Px}$  will primarily be used in deterministic design flood estimation methods, which consider only the average catchment conditions, with the average land-use changes and utilisation reflected by means of weighted runoff coefficients and/or curve number (CN) values. Simas (1996) included weighted CN values as land-use-related variables to estimate lag times in small to medium catchments ( $A \leq 15 \text{ km}^2$ ). However, Gericke and Smithers (2016) argued that weighted CN values represent a linear catchment response and suggested that MAP values should rather be used as a predictor variable to represent the regional rainfall variability, which potentially has a larger influence on any non-linearity present in the catchment response.

The combined use of the three methods, that is, duration of total net rise of a multi-peaked hydrograph (Equation 1), triangular-shaped direct runoff hydrograph approximation (Equation 4), and linear catchment response function (Equation 5), to estimate individual  $T_{Pxi}$  and/or catchment  $T_{Px}$  values in the four climatologically different regions of SA ensured that the high variability of event-based catchment responses is taken into account. However, the wider application of these three methods must also be contextualised in terms of other international medium to large catchment response time studies. For example, Pullen (1969), Mimikou (1984), and Thomas et al. (2000) used a simplified conventional convolution process to estimate the time parameters from observed rainfall and streamflow data in catchment areas in excess of  $5,000 \text{ km}^2$ . Pullen (1969) expressed  $T_L$  as the time from the centroid of effective rainfall to the centroid of a unit hydrograph. Mimikou (1984) used a multiperiod technique resulting in standardised storm duration hyetographs and corresponding unit hydrographs, with  $T_L$  being expressed as the time from the centroid of effective rainfall to the peak discharge. Thomas et al. (2000) expressed  $T_C$  as the time between the end of a rainfall event and the inflection point on the recession limb of a hydrograph. According to McCuen (2009), the centroid values used in the above-mentioned studies denote "average values" and are therefore considered to be more stable time variables, but Hood et al. (2007), on the other hand, emphasised the difficulty in estimating the centroid values of hyetographs and hydrographs at these catchment scales. Furthermore, the unit hydrograph theory is regarded to be more applicable to single-peaked hydrographs in smaller catchments (USDA NRCS, 2010). McCuen (2009) showed that the  $T_C$  definition adopted by Thomas et al. (2000) proved to be the less accurate (relative standard errors up to 20%) in comparison to the other three definitions used to estimate  $T_C$  from observed hyetographs and hydrographs.

Thus, by using the new approach developed in this study, both multi-peaked hydrographs (Equation 1) and triangular-shaped direct runoff hydrograph approximations (Equation 4) are included. Ultimately, Equation 4, which reflects the actual percentage of direct runoff under the rising limb of each individual hydrograph, can also be used in future to expand the unit hydrograph theory to larger catchments. In other words, the variable hydrograph shape parameter (Equation 4a) which reflects the actual percentage of direct runoff under the rising limb of each individual hydrograph can be used instead of the fixed volume of 37.5% normally associated with the conceptual curvilinear unit hydrograph theory.

The averages of Equations 1 and 4, which showed a high degree of association ( $r^2 > 0.97$ ) with Equation 5 (cf., Tables 2a to 2d), not only concluded the final screening process, but it also confirmed that catchment response times based on an assumed linear catchment response function (Equation 5) could provide results comparable to the sample mean of all the individual response times as estimated using Equations 1 and 4. Therefore, the application of Equation 5 is regarded to result in a useful "representative value" to ensure that the average of individual  $T_{Pxi}$  values is a good reflection of the catchment conditions and sample mean.

## 7 | CONCLUSIONS

The new and consistent approach developed in this study to derive the catchment  $T_{Px}$  in medium to large catchments in SA using only observed streamflow data proved to be both practical and objective with consistent results. The combined use of Equations 1, 4, and 5 not only ensured that the high variability of event-based catchment responses is taken into account, but the estimated catchment  $T_{Px}$  values are also well within the range of other uncertainties inherent to all design flood estimation procedures. It is recommended that for design hydrology and for the calibration of empirical time parameter equations that the catchment  $T_{Px}$  should be estimated using Equation 5. The fact that Gericke and Smithers (2016) successfully used the observed  $T_{Px}$  values (Equation 5) obtained from this study to derive new empirical time parameter equations, which resulted in improved estimates of peak discharge at a catchment level, confirms the application and merits of the new methodology.

For us to address the lack of appropriate methods used internationally to estimate catchment response times using an indirect or an empirical approach in ungauged catchments, the methodology developed in this study could be applied internationally in medium to large gauged catchments to directly derive realistic estimates of observed catchment response times from streamflow data, which has not been available previously. This will enable the derivation of new catchment and regional specific empirical time parameter equations to estimate the catchment response times in ungauged medium to large catchments. Thus, taking into consideration, the significant influence time parameter values have on the resulting hydrograph shape and peak discharge, the availability of observed catchment responses from medium to large catchments will facilitate new knowledge and enhance the understanding of hydrological processes at these catchment scales to ultimately provide improved peak discharge estimates.

## ACKNOWLEDGMENTS

Support for this research by the National Research Foundation (NRF), University of KwaZulu-Natal (UKZN), and Central University of Technology, Free State (CUT FS) is gratefully acknowledged. We also wish to thank the anonymous reviewers for their constructive review comments, which have helped to significantly improve the paper.

## REFERENCES

- Alexander, W. J. R. (2002). The standard design flood. *Journal of the South African Institution of Civil Engineering*, 44(1), 26–30.
- Arnold, J. G., Allen, P. M., Muttiah, R., & Bernhardt, G. (1995). Automated baseflow separation and recession analysis techniques. *Ground Water*, 33(6), 1010–1018.
- Balme, M., Vischel, T., Level, T., Peugeot, C. & Galle, S. (2006). Assessing the water balance in the Sahel: impact of small scale rainfall variability on runoff. Part 1: Rainfall variability analysis. *Journal of Hydrology* 331 (1–2): 336–348. doi:10.1016/j.jhydrol.2006.05.020
- Bondelid, T. R., McCuen, R. H., & Jackson, T. J. (1982). Sensitivity of SCS models to curve number variation. *Water Resources Bulletin*, 20(2), 337–349.
- Chapman, T. (1999). A comparison of algorithms for streamflow recession and baseflow separation. *Hydrological Processes*, 13, 701–714.
- Chow, V. T., Maidment, D. R., & Mays, L. W. (1988). *Applied hydrology*. New York: McGraw-Hill.
- Du Plessis, D. B. (1984). *Documentation of the March-May 1981 floods in the South Eastern Cape*. Pretoria: Department of Water Affairs and Forestry; Technical Report No. TR120.
- DWAF (1995). *GIS data: drainage regions of South Africa*. Pretoria: Department of Water Affairs and Forestry.
- Gericke, O. J., & Smithers, J. C. (2014). Review of methods used to estimate catchment response time for the purpose of peak discharge estimation. *Hydrological Sciences Journal*, 59(11), 1935–1971. doi:10.1080/02626667.2013.866712
- Gericke, O.J., & Smithers, J.C. (2015). An improved and consistent approach to estimate catchment response time: Case study in the C5 drainage region, South Africa. *Journal of Flood Risk Management*. doi:10.1111/jfr3.12206
- Gericke, O.J. & Smithers, J.C. (2016). Derivation and verification of empirical catchment response time equations for medium to large catchments in South Africa. *Hydrological Processes*. doi:10.1002/hyp.10922
- Görgens, A. H. M. (2007). *Joint peak-volume (JPV) design flood hydrographs for South Africa*. Pretoria: WRC Report No. 1420/3/07, Water Research Commission.
- Görgens, A. H. M., Lyons, S., Hayes, L., Makhabane, M., & Maluleke, D. (2007). *Modernised South African design flood practice in the context of dam safety*. Pretoria: WRC Report No. 1420/2/07, Water Research Commission.
- Hiemstra, L. A., & Francis, D. M. (1979). *The Runhydrograph: theory and application for flood predictions*. Pretoria: Water Research Commission.
- Hood, M.J., Clausen, J.C. & Warner, G.S. (2007). Comparison of stormwater lag times for low impact and traditional residential development. *Journal of the American Water Resources Association*, 43(4), 1036–1046. doi:10.1111/j.1752-1688.2007.00085.x
- HRU (1972). *Design flood determination in South Africa*. Johannesburg: Report No. 1/72, Hydrological Research Unit, University of the Witwatersrand.
- Hughes, D. A., Hannart, P., & Watkins, D. (2003). Continuous baseflow from time series of daily and monthly streamflow data. *WaterSA*, 29(1), 43–48.
- Johnstone, D. & Cross, WP. (1949). *Elements of applied hydrology*. New York: Ronald Press.
- Kadoya, M. & Fukushima, A. (1979). *Concentration time of flood runoff in smaller river basins*. In *Proceedings, 3<sup>rd</sup> International Hydrology Symposium on Theoretical and Applied Hydrology*. Morel-Seytoux HJ, Salas JD, Sanders TG and Smith RE (eds). Fort Collins, Colorado: Water Resources Publication; 75–88.
- Kirpich, Z. P. (1940). Time of concentration of small agricultural watersheds. *Civil Engineering*, 10(6), 362.
- Linsley, R. K., Kohler, M. A., & Paulhus, J. L. H. (1988). *Hydrology for Engineers*. SI metric. Singapore: McGraw-Hill.
- Lorenz, C. & Kunstmann, H. (2012). The hydrological cycle in three state-of-the-art reanalyses: intercomparison and performance analysis. *Journal of Hydrometeorology*, 13, 1397–1420. doi:10.1175/JHM-D-11-088.1
- Loukas, A. & Quick, MC. (1996). Physically-based estimation of lag time for forested mountainous watersheds. *Hydrological Sciences Journal*, 41(1), 1–19. doi:10.1080/02626669609491475
- Lynch, S. D. (2004). *Development of a raster database of annual, monthly and daily rainfall for Southern Africa*. Pretoria: WRC Report No. 1156/1/04, Water Research Commission.
- McCuen, R. H. (2005). *Hydrologic analysis and design* (3rd ed.). New York: Prentice-Hall.
- McCuen, R. H. (2009). Uncertainty analyses of watershed time parameters. *Journal of Hydrologic Engineering*, 14(5), 490–498.
- McCuen, R. H., Wong, S. L., & Rawls, W. J. (1984). Estimating urban time of concentration. *Journal of Hydraulic Engineering*, 110(7), 887–904.
- Midgley, D. C., Pitman, W. V., & Middleton, B. J. (1994). *Surface water resources of South Africa*. Pretoria: WRC Report No. 298/2/94, Water Research Commission.
- Mimikou, M. (1984). Regional relationships between basin size and runoff characteristics. *Hydrological Sciences Journal*, 29(1, 3), 63–73.
- Nathan, R. J., & McMahon, T. A. (1990). Evaluation of automated techniques for baseflow and recession analyses. *Water Resources Research*, 26(7), 1465–1473.
- Papadakis, K. N., & Kazan, M. N. (1987). Time of concentration in small rural watersheds. In *Proceedings, ASCE engineering hydrology symposium*. (pp. 633–638). Williamsburg, VA: ASCE.
- Pegram, G. G. S., & Parak, M. (2004). A review of the regional maximum flood and rational formula using geomorphological information and observed floods. *Water SA*, 30(3), 377–392.
- Pitman, W.V. (2011). Overview of water resource assessment in South Africa: Current state and future challenges. *WaterSA*, 37(5), 659–664. doi:10.4314/wsa.v37i5.3
- Pullen, R. A. (1969). *Synthetic Unitgraphs for South Africa*. Johannesburg: Report No. 3/69, Hydrological Research Unit, University of the Witwatersrand.
- Ramsbottom, D. M., & Whitlow, C. D. (2003). *Extension of Rating Curves at Gauging Stations Best Practice Guidance Manual*. R&D manual W6–061/M. Bristol: Environment Agency and HR Wallingford Limited.
- Rao, A. R., & Delleur, J. W. (1974). Instantaneous unit hydrograph, peak discharges and time lags in urban areas. *Hydrological Sciences Bulletin*, 19(2), 85–198. doi:10.1080/02626667409493898
- Royappen, M., Dye, P. J., Schulze, R. E., & Gush, M. B. (2002). *An analysis of catchment attributes and hydrological response characteristics in a range of small catchments*. Pretoria: WRC Report No. 1193/01/02, Water Research Commission.
- Sabol, G. V. (2008). *Hydrologic Basin response parameter estimation guidelines*. Scottsdale, Colorado: Dam Safety Report, Tierra Grande International Incorporated.
- SANRAL (2013). *Drainage manual* (6th ed.). Pretoria: South African National Roads Agency Limited.
- Schmidt, E. J., & Schulze, R. E. (1984). *Improved estimation of peak flow rates using modified SCS lag equations*. Pietermaritzburg: ACRU Report No. 17, Department of Agricultural Engineering, University of Natal.
- Seybert, T. A. (2006). *Stormwater Management for Land Development: methods and calculations for quantity control*. Hoboken, New Jersey: John Wiley and Sons Incorporated.

- Simas, M. J. C. (1996). *Lag time characteristics in small watersheds in the United States*. Thesis (PhD): University of Arizona.
- Smakhtin, V. U. (2001). Low flow hydrology: A review. *Journal of Hydrology*, 240(2001), 147–186.
- Smakhtin, V.U. & Watkins, D.A. (1997). *Low Flow estimation in South Africa*. Pretoria: WRC Report No. 494/1/97, Water Research Commission.
- Smithers, J. C., Gørgens, A. H. M., Gericke, O. J., Jonker, V., & Roberts, P. (2014). *The initiation of a National Flood Studies Programme for South Africa*. Pretoria: SANCOLD.
- Thomas, W. O., Monde, M. C., & Davis, S. R. (2000). Estimation of time of concentration for Maryland streams. *Journal of the Transportation Research Board*, 1720, 95–99.
- USDA NRCS. (2010). Time of concentration. In D.E. Woodward, C.C. Hoefft, A. Humpal & G. Cerrelli (Eds.), *National Engineering Handbook*. Washington, DC: United States Department of Agriculture Natural Resources Conservation Service; 1–18. Ch. 15 (Section 4, Part 630).
- USDA SCS (1985). Hydrology. In K. M. Kent, et al. (Eds.), *National Engineering Handbook*. Washington, DC: United States Department of Agriculture Soil Conservation Service; Section 4.
- USGS. (2002). SRTM topography [online]. United States Geological Survey. Available from: <http://dds.cr.usgs.gov/srtm/version2.1/SRTM/Document/Topo.pdf>. [2 June 2010].
- Watt, W. E., & Chow, K. C. A. (1985). A general expression for basin lag time. *Canadian Journal of Civil Engineering*, 12, 294–300.

**How to cite this article:** Gericke OJ, Smithers JC. Direct estimation of catchment response time parameters in medium to large catchments using observed streamflow data. *Hydrological Processes*. 2017;31:1125–1143. <https://doi.org/10.1002/hyp.11102>

## APPENDIX A

Simple linear regression is used as estimation technique to derive the linear catchment response function (Equation 5) as discussed in the Methodology. The linear regression model determines how the catchment  $T_{Px}$  value (dependent variable), on average, is affected by the independent variables, that is, the observed peak discharge ( $Q_{Pxi}$ ,  $m^3 s^{-1}$ ) and direct runoff volume ( $Q_{Dxi}$ ,  $m^3$ ) values as obtained from individual flood hydrographs.

In other words, the slope of the assumed linear catchment response function in Equation 5 depicts the rate of change between corresponding  $Q_{Pxi}$  and  $Q_{Dxi}$  values along the linear regression and equals the average catchment  $T_{Px}$  value by considering all the individual  $Q_{Pxi}$  and  $Q_{Dxi}$  values in a particular catchment. In essence, the best-fit line is fitted through a scatter plot of the  $Q_{Pxi}$  and  $Q_{Dxi}$  values in such a way that the sum of squared residuals ( $Z$ ), that is,  $Z$  in  $Q_{Dx}$ ,  $\sum (Q_{Dxi} - \hat{Q}_{Dxi})^2$  is minimised.

The best-fit line fitted through a scatter plot of the  $Q_{Pxi}$  and  $Q_{Dxi}$  values is given by

$$\hat{Q}_{Dxi} = T_{Px} Q_{Pxi} + c, \quad (A1)$$

By substituting Equation A1, the sum of squared residuals ( $Z$ ) is given by

$$Z = \sum_{i=1}^N (Q_{Dxi} - T_{Px} Q_{Pxi} - c)^2, \quad (A2)$$

By minimising  $Z$  for the values of  $c$  and  $T_{Px}$ , then  $\partial Z / \partial c = 0$  and  $\partial Z / \partial T_{Px} = 0$ .

First condition ( $c = y$ -intercept = 0):

$$\begin{aligned} \frac{\partial Z}{\partial c} &= \sum_{i=1}^N -2(Q_{Dxi} - c - T_{Px} Q_{Pxi}), \\ &= 2 \left( Nc + T_{Px} \sum_{i=1}^N Q_{Pxi} - \sum_{i=1}^N Q_{Dxi} \right) = 0, \quad (A3) \end{aligned}$$

By dividing Equation A3 with 2 and solving for the  $y$ -intercept ( $c$ ):

$$c = \overline{Q_{Dx}} - T_{Px} \overline{Q_{Px}}, \quad (A4)$$

Equation A4 indicates that the constant  $c$  ( $y$ -intercept) is set such that the linear regression line go through the mean of the  $Q_{Pxi}$  and  $Q_{Dxi}$  values, respectively.

Second condition ( $T_{Px} = \text{slope} = 0$ ):

$$\begin{aligned} \frac{\partial Z}{\partial T_{Px}} &= \sum_{i=1}^N -2Q_{Pxi}(Q_{Dxi} - c - T_{Px} Q_{Pxi}), \\ &= \sum_{i=1}^N -2(Q_{Pxi} Q_{Dxi} - c Q_{Pxi} - T_{Px} Q_{Pxi}^2) = 0, \quad (A5) \end{aligned}$$

By substituting the expression for the  $y$ -intercept ( $c$ ) from Equation A4 into Equation A5, then

$$\sum_{i=1}^N (Q_{Pxi} Q_{Dxi} - Q_{Pxi} \overline{Q_{Dx}} + T_{Px} Q_{Pxi} \overline{Q_{Px}} - T_{Px} Q_{Pxi}^2) = 0, \quad (A6)$$

Equation A6 can be separated into two sums:

$$\sum_{i=1}^N (Q_{Pxi} Q_{Dxi} - Q_{Pxi} \overline{Q_{Dx}}) - T_{Px} \sum_{i=1}^N (Q_{Pxi}^2 - Q_{Pxi} \overline{Q_{Px}}) = 0, \quad (A7)$$

Then, Equation A7 becomes directly

$$\begin{aligned} T_{Px} &= \frac{\sum_{i=1}^N (Q_{Pxi} Q_{Dxi} - Q_{Pxi} \overline{Q_{Dx}})}{\sum_{i=1}^N (Q_{Pxi}^2 - Q_{Pxi} \overline{Q_{Px}})}, \\ &= \frac{\sum_{i=1}^N (Q_{Pxi} Q_{Dxi}) - N \overline{Q_{Px}} \overline{Q_{Dx}}}{\sum_{i=1}^N (Q_{Pxi}^2) - N \overline{Q_{Px}}^2}, \quad (A8) \end{aligned}$$

Equation A8 can be translated into more intuitively obvious forms, by noting that

$$\sum_{i=1}^N (\overline{Q_{Px}}^2 - Q_{Pxi} \overline{Q_{Px}}) = 0, \quad \text{and} \quad (A9)$$

$$\sum_{i=1}^N (\overline{Q_{Px}} \overline{Q_{Dx}} - Q_{Dxi} \overline{Q_{Px}}) = 0, \quad (A10)$$

Therefore, by considering both Equations A9 and A10,  $T_{Px}$  can be rewritten as the ratio of

$$T_{P_x} = \frac{\text{Cov}(Q_{P_x}, Q_{D_x})}{\text{Var}(Q_{P_x})},$$

$$T_{P_x} = \left[ \frac{\sum_{i=1}^N (Q_{P_{xi}} - \overline{Q_{P_x}})(Q_{D_{xi}} - \overline{Q_{D_x}})}{\sum_{i=1}^N (Q_{P_{xi}} - \overline{Q_{P_x}})^2} \right], \quad (\text{A11})$$

By converting the resulting time units from seconds to hours and incorporating a variable proportionality ratio (default  $x = 1$ ), then Equation A11 becomes

$$T_{P_x} = \frac{1}{3600x} \left[ \frac{\sum_{i=1}^N (Q_{P_{xi}} - \overline{Q_{P_x}})(Q_{D_{xi}} - \overline{Q_{D_x}})}{\sum_{i=1}^N (Q_{P_{xi}} - \overline{Q_{P_x}})^2} \right], \quad (\text{A12})$$

where  $T_{P_x}$  is the average catchment time to peak based on a linear catchment response function (h),  $Q_{D_{xi}}$  is the volume of direct runoff for individual flood events ( $\text{m}^3$ ),  $\hat{Q}_{D_{xi}}$  is the predicted value from the least-squares line of  $Q_{D_{xi}}$  on  $Q_{P_{xi}}$  ( $\text{m}^3$ ),  $\overline{Q_{D_x}}$  is the mean of  $Q_{D_{xi}}$  ( $\text{m}^3$ ),  $Q_{P_{xi}}$  is the observed peak discharge for individual flood events ( $\text{m}^3 \text{ s}^{-1}$ ),  $\overline{Q_{P_x}}$  is the mean of  $Q_{P_{xi}}$  ( $\text{m}^3 \text{ s}^{-1}$ ),  $c$  is the  $y$ -intercept,  $N$  is the sample size,  $x$  is the variable proportionality ratio (default  $x = 1$ ), which depends on the catchment response time parameter under consideration, and  $Z$  is the sum of squared residuals.

It is important to note that Equation A12 represents Equation 5. As highlighted in the Methodology, the variable proportionality ratio ( $x$ ) is included in Equation A12 and/or Equation 5 to increase the flexibility and use thereof, that is, with  $x = 1$ , either  $T_{P_x}$  or  $T_{C_x}$  could be estimated by acknowledging the approximation of  $T_C \approx T_P$  (Gericke and Smithers, 2014) and with  $x = 1.667$ ,  $T_L$  could be estimated by assuming that  $T_L = 0.6T_C$ , which is the time from the centroid of effective rainfall to the time of peak discharge (McCuen, 2009).